A NUMERICAL ANALYSIS OF NONCIRCULAR CYLINDRICAL SHELLS

By

JIMMIE D. RAMEY

Bachelor of Science
Oklahoma State University
Stillwater, Oklahoma
1960

Master of Science
Oklahoma State University
Stillwater, Oklahoma
1962

Submitted to the faculty of the Graduate College
of the Oklahoma State University
in partial fulfillment of the requirements
for the Degree of
DOCTOR OF PHILOSOPHY
August, 1969

A NUMERICAL ANALYSIS OF NONCIRCULAR

CYLINDRICAL SHELLS

Thesis Approved:

Harold E. Boyd
Thesis Adviser

James V. Parker

Robert H. Gibson

D. D. Durham
Dean of the Graduate College

ACKNOWLEDGMENTS

The author wishes to express his gratitude and sincere appreciation to the following individuals and organizations:

To Professor Donald E. Boyd for guidance and friendship and his assistance as the writer's adviser in the preparation of this thesis;

To the members of his advisory committee, Donald E. Boyd, James V. Parcher, Ahmed E. Salama, Robert W. Gibson, for their guidance and encouragement;

To the Civil Engineering Department at Oklahoma State University and the U.S. Department of Health, Education, and Welfare, for providing the opportunity for financial assistance.

To his wife, Alice, and his children, Jimmie and Mary, for their patient understanding, encouragement and many sacrifices during this undertaking;

To Mr. Eldon Hardy for preparing the final sketches;

To Mrs. Mary Ann Kelsey for typing the final manuscript.

Jimmie D. Ramey

August, 1969

Stillwater, Oklahoma

TABLE OF CONTENTS

LIST OF TABLES

LIST OF FIGURES

NOMENCLATURE

$[A]$	Matrix of finite difference coefficients relating the forces and deflections
a,b	Semi-minor and semi-major axes of an ellipse
c	$12\left(\frac{r}{h}\right)^2\left\{\frac{r}{h}\log\left[\frac{1+\frac{h}{2r}}{1-\frac{h}{2r}}-1\right]\right\}$
D	$\frac{Eh}{1-\nu^2}$
E	Modulus of elasticity
h	Shell thickness
i,j	Finite difference grid variables in x and s directions
K	$\frac{Eh^3}{12(1-\nu^2)}$
L, ℓ	Length of shell in x and s-directions
M_x, M_s	Bending moment stress resultants
M_{xs}, M_{sx}	Twisting moment stress resultants
N_x, N_s	Membrane stress resultants
N_{xs}, N_{sx}	Shearing stress resultants
$\{P\}$	Grid point forces
P_x, P_s, P_z	Load intensity in x, s, and z directions
$\overline{P}_x$	$\frac{P_x}{D}$

$\overline{P}_s$	$\frac{P_s}{D}$
$\overline{P}_z$	$\frac{P_z}{K}$
$\overline{P}_\zeta$	$-(1-\nu^2)\left(\frac{\ell}{h}\right)^2 \frac{P_x}{P_z}$
$\overline{P}_\eta$	$-(1-\nu^2)\left(\frac{\ell}{h}\right)^2 \frac{P_s}{P_z}$
$\overline{P}_r$	$12(1-\nu^2)\left(\frac{\ell}{h}\right)^4$
Q_x, Q_s	Transverse shear resultants
r	Radius of circular shells
r_j	Radius of noncircular shells at finite difference grid line j
s, x, z	Spatial coordinates
T_{xs}, T_{sx}, V_x, V_s	Kirchoff shear resultants
u, v, w	Orthogonal displacements
$\overline{u}$, $\overline{v}$, $\overline{w}$	Nondimensional orthogonal displacements $\frac{Eu}{P_z h}$, $\frac{Ev}{P_z h}$, $\frac{Ew}{P_z h}$
α	$\frac{\beta\ell}{2}$
β	$\left(\frac{Eh}{4r^2K}\right)^{1/4}$
β_x, β_s, β_{xs}	Slopes and twist of deformed element
$\Delta\zeta$, $\Delta\eta$	Finite difference grid spaces
$\{\delta\}$	Grid point deflections
ε_x, ε_s, ε_{xs}, ε_{sx}	Normal and shearing strains
ζ, η	Nondimensional spatial coordinates $\frac{x}{L}$, $\frac{s}{\ell}$

θ	Subtended angle for circular segment
ν	Poisson's Ratio
ξ	Noncircularity parameter
σ_x , σ_s	Normal stresses
τ_{xs} , τ_{sx}	Shearing stresses
ω_x , ω_s , ω_z	Median surface rotations

CHAPTER I

INTRODUCTION

1.1 Discussion and Background

The widespread use of thin shell structures has created a need for a systematic method of analysis which can adequately account for arbitrary geometric form and boundary conditions as well as variable thickness and anisotropic material properties. Classical thin shell theory yields differential equations of equilibrium or continuity whose complexity depends greatly on the shell geometry and whose solution depends on the geometric configuration of the boundary and the type of force or displacement quantity which must be satisfied there. Therefore, classical solutions are available only for simple geometric forms whose boundaries coincide with the parametric curves that describe the shell surface. In this context the sphere and the circular cylinder are amenable to classical solutions and have been studied extensively.

Many times, especially in the aircraft and aerospace industry, the engineer is faced with the problem of analyzing cylindrical shells which are not circular. Shells of this type do not easily lend themselves to a classical solution. Oval fuselage sections are examples of closed, noncircular cylindrical shells. Skin panels between wing stringers, spars, and ribs are examples of open, noncircular cylindrical shells. Whether the reference is to closed cylinders or to open cylinders, most stressed-skin structures employ many noncircular shell

elements. The literature contains relatively few investigations of noncircular cylindrical shells.

Kempner (1) derived energy expressions and differential equations useful in stress and displacement analyses of noncircular cylindrical shells. These equations are equivalent to the equations Flugge (2) derived for the circular cylindrical shells. Subsequently, Kempner and his students performed a series of investigations into a class of short oval cylinders using a simplified system of equations equivalent to the well known Donnell equations (3).

These oval cylinders are characterized by radii of curvature which vary around the circumference of the shells according to a simple mathematical expression containing an "eccentricity" parameter. Their studies, which have continued to date, have contributed significantly to the knowledge of the static behavior of closed cylindrical shells.

Boyd (4) developed a method for the analysis of arbitrary, open cylindrical shells using the simplified system of shell equations equivalent to Donnell's (3) equations. These equations are believed to be reasonably accurate for shell segments resembling a curved thin plate (such as a typical skin panel). Boyd's (4) work resulted in a method of small displacement and stress analysis for a constant-thickness, cylindrical shell segment characterized by arbitrary curvature variation around the circumference, arbitrary boundary conditions along the straight edges of the segment, and arbitrary normal pressures distributed over the surface.

These investigations, including those by Kempner's students were primarily concerned with the analysis of short, noncircular cylindrical shells, and made extensive use of the Donnell equations. While such

analyses are considerably simpler than those based on the more accurate equations derived by Kempner (1), they provide no reliable information concerning the displacement and stress analysis of the longer shells. In this study two aspects of the problem of noncircular cylindrical shells are considered. One of these is to develop a numerical procedure for the solution of the Flugge equations as derived by Kempner (1). The other aspect is to compare the accuracy of the Donnell equations for noncircular cylindrical shells to the Flugge equations for noncircular cylindrical shells.

1.2 Approach

The differential equations of equilibrium derived by Kempner (1) were used as the basis of this study. The derivatives of the displacements u, v, and w were replaced by finite-difference quotients in order to reduce the linear differential equations to a set of linear algebraic equations. The closed, noncircular cylindrical shell (Figure 1) and its loading are assumed to be symmetrical with respect to the midplanes ($s = 0$ and $s = \ell/4$) and with respect to the center line of the shell ($x = 0$). This allows an analysis to be performed by considering only one-eighth of the shell (shown with the 8 x 8 finite difference grid layout superimposed on the shell surface (Figure 1).) The closed cylinders are assumed to be simply supported (s.s.) on the two ends. Full advantage is taken of the assumed symmetry.

An open circular cylindrical shell is analyzed as an example. This shell (Figure 2) is assumed to be symmetrical with respect to the center line of the shell ($x = 0$), and is assumed to be simply supported (s.s.) along the curved edges and pinned supported (p.s.) along the

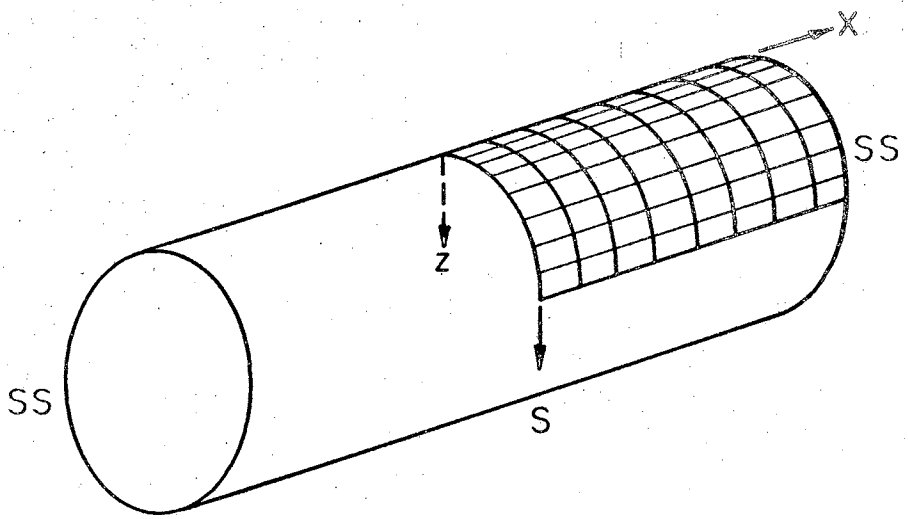

Figure 1. Closed Noncircular Cylindrical Shell

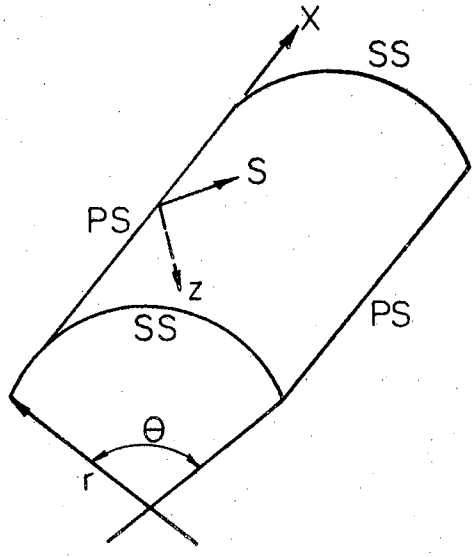

Figure 2. Open Circular Cylindrical Shell

straight edges.

Once the linear algebraic equations are obtained, the solution for the unknown displacements u, v, and w are obtained by solving the set of equations using the Gauss-Jordon (5) technique.

CHAPTER II

FORMULATION OF THE SOLUTION

2.1 Equilibrium Equations

The equations of equilibrium governing the deformation of noncircular cylindrical shells are given by Kempner (1). For completeness the derivation is duplicated in Appendix A and given again by the following three equations:

$$u_{,xx} + \frac{1-\nu}{2} u_{,ss} + \frac{1+\nu}{2} v_{,xs} - \frac{\nu}{r} w_{,x}$$

$$+ \frac{h^2}{12r} w_{,xxx} - \left[\frac{h^2(1-\nu)}{24r} w_{,xs}\right]_{,s} + \left[\frac{h^2(1-\nu)}{24r^2} u_{,s}\right]_{,s} = \bar{P}_x$$

$$v_{,ss} + \frac{1-\nu}{2} v_{,xx} + \frac{1+\nu}{2} u_{,xs} - \left(\frac{w}{r}\right)_{,s} + \frac{h^2(1-\nu)}{8r^2} v_{,xx}$$

$$+ \frac{h^2(3-\nu)}{24r} w_{,xxs} + \frac{h^2}{12r^2} r_{,s} w_{,ss} + \frac{h^2}{12r^2} r_{,s} \frac{w}{r^2} - \frac{h^2}{12r^2} \frac{r_{,s}^2}{r^2} v = \bar{P}_s$$

$$w_{,xxxx} + 2w_{,xxss} + w_{,ssss} + \frac{1}{r^2} w_{,ss} + \left(\frac{w}{r^2}\right)_{,ss} + \frac{w}{r^4} + \frac{1}{r} u_{,xxx}$$

$$-\frac{1-\nu}{2}\left(\frac{v_{,xs}}{r}\right)_{,s}+\frac{3-\nu}{2}\left(\frac{v_{,xx}}{r}\right)_{,s}-\left(\frac{r_{,s}v}{r^2}\right)_{,ss}$$

$$-\left(\frac{r_{,s}}{r^4}\right)v-\frac{12}{h^2r}V_{,s}+\frac{12w}{h^2r^2}-\frac{12}{h^2r}u_{,x}=\overline{P}_z \qquad (2.1)$$

where subscripts following a comma indicate differentiation. From Figures 1 and 16.

x, s, z = longitudinal, circumferential, and transverse spatial coordinates, respectively.

u, v, w = displacements in the x, s, z directions, respectively.

r = variable radius of curvature.

ν = Poisson's ratio.

h = shell thickness (assumed constant)

$$\overline{P}_x = -\frac{(1-\nu^2)}{Eh}P_x$$

$$\overline{P}_s = -\frac{(1-\nu^2)}{Eh}P_s$$

$$\overline{P}_z = \frac{12(1-\nu^2)}{Eh^3}P_z$$

P_x, P_s, and P_z = Loading intensity applied to the median surface of the shell in the x, s, and z directions, respectively.

Equations 2.1 may be rewritten in nondimensional form by using the following nondimensional parameters:

$$\zeta = \frac{x}{L}$$

$$\eta = \frac{s}{\ell} \qquad (2.2)$$

where

L = length of cylinder in x-direction,

ℓ = arc length of cylinder in s-direction.

In nondimensional form equations 2.1 become

$$\left(\frac{\ell}{L}\right)^2 \bar{u}_{,\zeta\zeta} \frac{1-\nu}{2} \bar{u}_{,\eta\eta} + \frac{1+\nu}{2}\left(\frac{\ell}{L}\right) \bar{v}_{,\zeta\eta} - \left(\frac{\ell}{r}\right)\left(\frac{\ell}{L}\right) \bar{w}_{,\zeta}$$

$$+ \frac{\left(\frac{\ell}{L}\right)^3 \left(\frac{\ell}{r}\right)}{12\left(\frac{\ell}{h}\right)^2} \bar{w}_{,\zeta\zeta\zeta} - \frac{(1-\nu)\frac{\ell}{L}}{24\left(\frac{\ell}{h}\right)^2} \left[\frac{\ell}{r} \bar{w}_{,\zeta\eta}\right]_{,\eta} + \frac{1-\nu}{12\left(\frac{\ell}{h}\right)^2} \left[\left(\frac{\ell}{r}\right)^2 \bar{u}_{,\eta}\right]_{,\eta} = \bar{P}_{\zeta}$$

$$\bar{v}_{,\eta\eta} + \frac{1-\nu}{2}\left(\frac{\ell}{L}\right)^2 \bar{v}_{,\zeta\zeta} + \frac{1+\nu}{2}\left(\frac{\ell}{L}\right) \bar{u}_{,\zeta\eta} - \left[\frac{\ell}{r} w\right]_{,\eta} + \frac{(1-\nu)\left(\frac{\ell}{L}\right)^2}{8\left(\frac{\ell}{h}\right)^2}\left(\frac{\ell}{r}\right)^2 \bar{v}_{,\zeta\zeta}$$

$$+ \frac{(3-\nu)\left(\frac{\ell}{L}\right)^2}{24\left(\frac{\ell}{h}\right)^2}\left(\frac{\ell}{r}\right) \bar{w}_{,\zeta\zeta\eta} + \frac{\left(\frac{\ell}{r}\right)^2\left(\frac{r}{\ell}\right)_{,\eta}}{12\left(\frac{\ell}{h}\right)^2} \bar{w}_{,\eta\eta} + \frac{\left(\frac{\ell}{r}\right)^4\left(\frac{r}{\ell}\right)_{,\eta}}{12\left(\frac{\ell}{h}\right)^2} \bar{w}$$

$$- \frac{\left(\frac{\ell}{r}\right)^4\left(\frac{r}{\ell}\right)_{,\eta}}{12\left(\frac{\ell}{h}\right)^2} \bar{v} = \bar{P}_{\eta}$$

$$\left(\frac{\ell}{L}\right)^4 \bar{w}_{,\zeta\zeta\zeta\zeta} + 2\left(\frac{\ell}{L}\right)^2 \bar{w}_{,\zeta\zeta\eta\eta} + \bar{w}_{,\eta\eta\eta\eta} + \left(\frac{\ell}{r}\right)^2 \bar{w}_{,\eta\eta} + \left[\left(\frac{\ell}{r}\right)^2 \bar{w}\right]_{,\eta\eta}$$

$$+ \left(\frac{\ell}{r}\right)^4 \bar{w} + \left(\frac{\ell}{L}\right)^3\left(\frac{\ell}{r}\right) \bar{u}_{,\zeta\zeta\zeta} - \frac{1-\nu}{2}\left[\left(\frac{\ell}{r}\right) \bar{v}_{,\zeta\eta}\right]_{,\eta} + \frac{3-\nu}{2}\left(\frac{\ell}{L}\right)^2 \left[\left(\frac{\ell}{r}\right) \bar{v}_{,\zeta\zeta}\right]_{,\eta}$$

$$- \left[\left(\frac{\ell}{r}\right)^2 \left(\frac{r}{\ell}\right)_{,\eta} \bar{v} \right]_{,\eta\eta} - \left(\frac{\ell}{r}\right)^4 \left(\frac{r}{\ell}\right)_{,\eta} \bar{v} - 12 \left(\frac{\ell}{h}\right)^2 \left(\frac{\ell}{r}\right) \bar{v}_{,\eta}$$

$$+ 12 \left(\frac{\ell}{h}\right)^2 \left(\frac{\ell}{r}\right)^2 \bar{w} - 12\nu \left(\frac{\ell}{h}\right)^2 \left(\frac{\ell}{L}\right)\left(\frac{\ell}{r}\right) \bar{u}_{,\zeta} = \bar{P}_r \qquad (2.3)$$

where

$$\left(\bar{u}, \bar{v}, \bar{w}\right) = \left(\frac{Eu}{P_z h}, \frac{Ev}{P_z h}, \frac{Ew}{P_z h}\right)$$

$$\bar{P}_\zeta = - (1 - \nu^2) \left(\frac{\ell}{h}\right)^2 \frac{P_x}{P_z}$$

$$\bar{P}_\eta = - (1 - \nu^2) \left(\frac{\ell}{h}\right)^2 \frac{P_s}{P_z}$$

$$\bar{P}_r = 12 (1 - \nu^2) \left(\frac{\ell}{h}\right)^4$$

Equation 2.3 is a set of three coupled partial differential equations with variable coefficients. As discussed in the Introduction, these equations will be solved using the finite difference technique (2.3).

2.2 Donnell's Equilibrium Equations

The equilibrium equations given by equations 2.1 are very cumbersome to apply to the solution of shell problems because of the laborious calculations which are associated with them. A somewhat simpler set of equations, which have met with fairly wide application, were derived by Donnell (3). By assuming that the transverse shearing force Q_s makes

a negligible contribution to the equilibrium of forces in the circumferential direction, and that the changes of curvature and twist are negligibly affected by the tangential displacement, v, the governing partial differential equations for a noncircular shell reduce to the set given by equations 2.4

$$u_{,xx} + \frac{1-\nu}{2} u_{,ss} + \frac{1+\nu}{2} v_{,xs} - \frac{\nu}{r} w_{,x} = \bar{P}_x$$

$$v_{,ss} + \frac{1-\nu}{2} v_{,xx} + \frac{1+\nu}{2} u_{,xs} - \left(\frac{w}{r}\right)_{,s} = \bar{P}_s$$

$$w_{,xxxx} + 2w_{xxss} + w_{,ssss}$$

$$- \frac{12}{h^2 r} v_{,s} + \frac{12}{h^2 r^2} w - \frac{12\nu}{h^2 r} u_{,x} = \bar{P}_z \qquad (2.4)$$

where the notation is the same as in 2.1.

Using the nondimensional parameters of equation 2.2 the nondimensional form of Donnell's equilibrium equations are

$$\left(\frac{\ell}{L}\right)^2 \bar{u}_{,\zeta\zeta} + \frac{1-\nu}{2} \bar{u}_{,\eta\eta} + \frac{1+\nu}{2}\left(\frac{\ell}{L}\right) \bar{v}_{,\zeta\eta} - \nu\left(\frac{\ell}{L}\right)\left(\frac{\ell}{r}\right) \bar{w}_{,\zeta} = \bar{P}_\zeta$$

$$\bar{v}_{,\eta\eta} + \frac{1-\nu}{2}\left(\frac{\ell}{L}\right)^2 \bar{v}_{,\zeta\zeta} + \frac{1+\nu}{2}\left(\frac{\ell}{L}\right) \bar{u}_{,\zeta\eta} - \left[\left(\frac{\ell}{r}\right) \bar{w}\right]_{,\eta} = \bar{P}_\eta$$

$$\left(\frac{\ell}{L}\right)^4 \bar{w}_{,\zeta\zeta\zeta\zeta} + 2\left(\frac{\ell}{L}\right)^2 \bar{w}_{,\zeta\zeta\eta\eta} + \bar{w}_{,\eta\eta\eta\eta}$$

$$- 12\left(\frac{\ell}{h}\right)^2\left(\frac{\ell}{r}\right) \bar{v}_{,\eta} + 12\left(\frac{\ell}{h}\right)^2\left(\frac{\ell}{r}\right)^2 \bar{w} - 12\nu\left(\frac{\ell}{h}\right)^2\left(\frac{\ell}{L}\right)\left(\frac{\ell}{r}\right) \bar{u}_{,\zeta} = \bar{P}_r \qquad (2.5)$$

Note that these equations are also a set of three coupled partial differential equations with variable coefficients. The accuracy of these simplified equations will be compared to that of Kempner's form of the Flugge equations.

2.3 Formulation of the Finite Difference Equations

The finite difference technique reduces the linear differential equations for a continuous system into a set of linear algebraic equations. Conventional algebraic equations, called finite-difference quotients, are used in place of the derivatives of the displacements.

The finite difference quotients used in this study are conventional central difference given by Salvadori (6) and given by Equations 2.6.

$$f_{,\zeta}\Big|_{i,j} = \frac{1}{2\Delta\zeta}\left[f_{i+1,j} - f_{i-1,j}\right]$$

$$f_{,\eta}\Big|_{i,j} = \frac{1}{2\Delta\eta}\left[f_{i,j+1} - f_{i,j-1}\right]$$

$$f_{,\zeta\zeta}\Big|_{i,j} = \frac{1}{\Delta\zeta^2}\left[f_{i+1,j} - 2f_{i,j} + f_{i-1,j}\right]$$

$$f_{,\eta\eta}\Big|_{i,j} = \frac{1}{\Delta\eta^2}\left[f_{i,j+1} - 2f_{i,j} + f_{i,j-1}\right] \qquad (2.6)$$

Note that the approximations are given in terms of an arbitrary point i,j on the shell middle surface. All the approximations needed to express the governing equations in finite difference form can be generated from those given by Equations 2.6. For completeness, the finite difference approximations used in this study are tabulated in Appendix B.

2.4 Boundary Conditions

In accordance with the discussion given by Kraus (7), four boundary conditions must be given for each edge of the shell. These boundary conditions for an open shell are:

for sides of constant x

$$\begin{array}{lcl} u = 0 & & N_x = 0 \\ v = 0 & & T_{sx} = 0 \\ & \text{OR} & \\ w = 0 & & V_x = 0 \\ \beta_x = 0 & & M_x = 0 \end{array} \qquad (2.7)$$

for sides of constant s

$$\begin{array}{lcl} u = 0 & & T_{xs} = 0 \\ v = 0 & & N_s = 0 \\ & \text{OR} & \\ w = 0 & & V_s = 0 \\ \beta_s = 0 & & M_s = 0 \end{array} \qquad (2.8)$$

where

β_x, β_s = the slope of the surface (Figure 21).

T, V = Kirchoff shears given by Equations 2.9

N, M = stress resultants given in Appendix A.

The Kirchoff shears are:

$$T_{sx} = N_{sx}$$

$$T_{xs} = N_{xs} + \frac{M_{xs}}{r}$$

$$V_x = Q_x + (M_{xs})_{,s}$$

$$V_s = Q_s + (M_{sx})_{,x} \tag{2.9}$$

where

Q, M = stress resultants given in Appendix A.

The boundary conditions for shells closed with respect to s are the same as those given by Equation 2.7.

In cases where the shell is symmetrical, closed, and symmetrically loaded, conditions of symmetry can be used to advantage. In this study two different sets of boundary conditions are used. First, for the closed shells it was assumed that the shell and its loading are symmetrical with respect to the generators at $\eta = 0$ and at $\eta = 1/4$; and symmetrical with respect to the circumference line at $\zeta = 0$. This allows an analysis to be performed using only one-eighth of the shell as shown by Figure 1. The boundary conditions used are:

$$\left.\begin{aligned} T_{xs} &= 0 \\ v &= 0 \\ V_s &= 0 \\ \beta_s &= 0 \end{aligned}\right\} \quad \text{For } \eta = 0 \text{ and } \eta = 1 \text{ with } 0 \leq \zeta \leq 1 \tag{2.10}$$

$$\left.\begin{aligned} u &= 0 \\ T_{sx} &= 0 \\ V_x &= 0 \\ \beta_x &= 0 \end{aligned}\right\} \quad \text{For } \zeta = 0 \text{ with } 0 \leq \eta \leq 1 \tag{2.11}$$

$$\left.\begin{aligned} N_x &= 0 \\ v &= 0 \\ w &= 0 \\ M_x &= 0 \end{aligned}\right\} \quad \text{For } \zeta = 1 \text{ with } 0 \leq \eta \leq 1 \tag{2.12}$$

In the case of open shells the boundary conditions used were:

$$\left.\begin{aligned} u &= 0 \\ v &= 0 \\ w &= 0 \\ M_s &= 0 \end{aligned}\right\} \quad \text{For } \eta = 0 \text{ and } \eta = 1 \text{ with } 0 \leq \zeta \leq 1 \tag{2.13}$$

Along sides of constant ζ, the boundary conditions are given by Equations 2.10 and 2.11.

In terms of displacements, the boundary conditions for the closed shell are:

$$\left.\begin{aligned} v &= 0 \\ u_{,\eta} &= 0 \\ w_{,\eta\eta\eta} &= 0 \\ w_{,\eta} &= 0 \end{aligned}\right\} \quad \text{For } \eta = 0 \text{ and } \eta = 1 \text{ with } 0 \leq \zeta \leq 1 \tag{2.14}$$

$$\left.\begin{aligned} u &= 0 \\ v &= 0 \\ w_{,\zeta} &= 0 \\ w_{,\zeta\zeta} &= 0 \end{aligned}\right\} \quad \text{For } \zeta = 0 \text{ with } 0 \leq \eta \leq 1 \tag{2.15}$$

$$\left.\begin{aligned} u,_{\zeta} &= 0 \\ v &= 0 \\ w &= 0 \\ w,_{\zeta\zeta} &= 0 \end{aligned}\right\} \quad \text{For } \zeta = 1 \text{ with } 0 \leq \eta \leq 1 \tag{2.16}$$

In terms of displacements, the boundary conditions for the open shell are:

$$\left.\begin{aligned} u &= 0 \\ v &= 0 \\ w &= 0 \\ w,_{\eta\eta} &= 0 \end{aligned}\right\} \quad \text{For } \zeta = 0 \text{ and } \zeta = 1 \text{ with } 0 \leq \eta \leq 1 \tag{2.17}$$

For $\zeta = 0$ and $\zeta = 1$ with $0 \leq \eta \leq 1$ the boundary conditions are, as before, the same as in the closed shell (Equations 2.15 and 2.16).

2.5 Application of Finite Difference Equations

The replacement of the continuous domain D by a pattern of discrete points within D is shown in Figure 3. As a result of the approximation, the solutions for u, v and w are not continuous solutions but are approximations to u, v and w at the isolated points (Figure 3).

The grid system used in this study is shown in Figure 4.

The equilibrium equations in finite difference form are applied at all interior points; i.e., at point p_{ij}, for $2 \leq i \leq 8$, and $2 \leq j \leq 8$; and at certain boundary points depending on the boundary conditions. For convenience in this study, the variables are renumbered with a single subscript as shown by Figure 5.

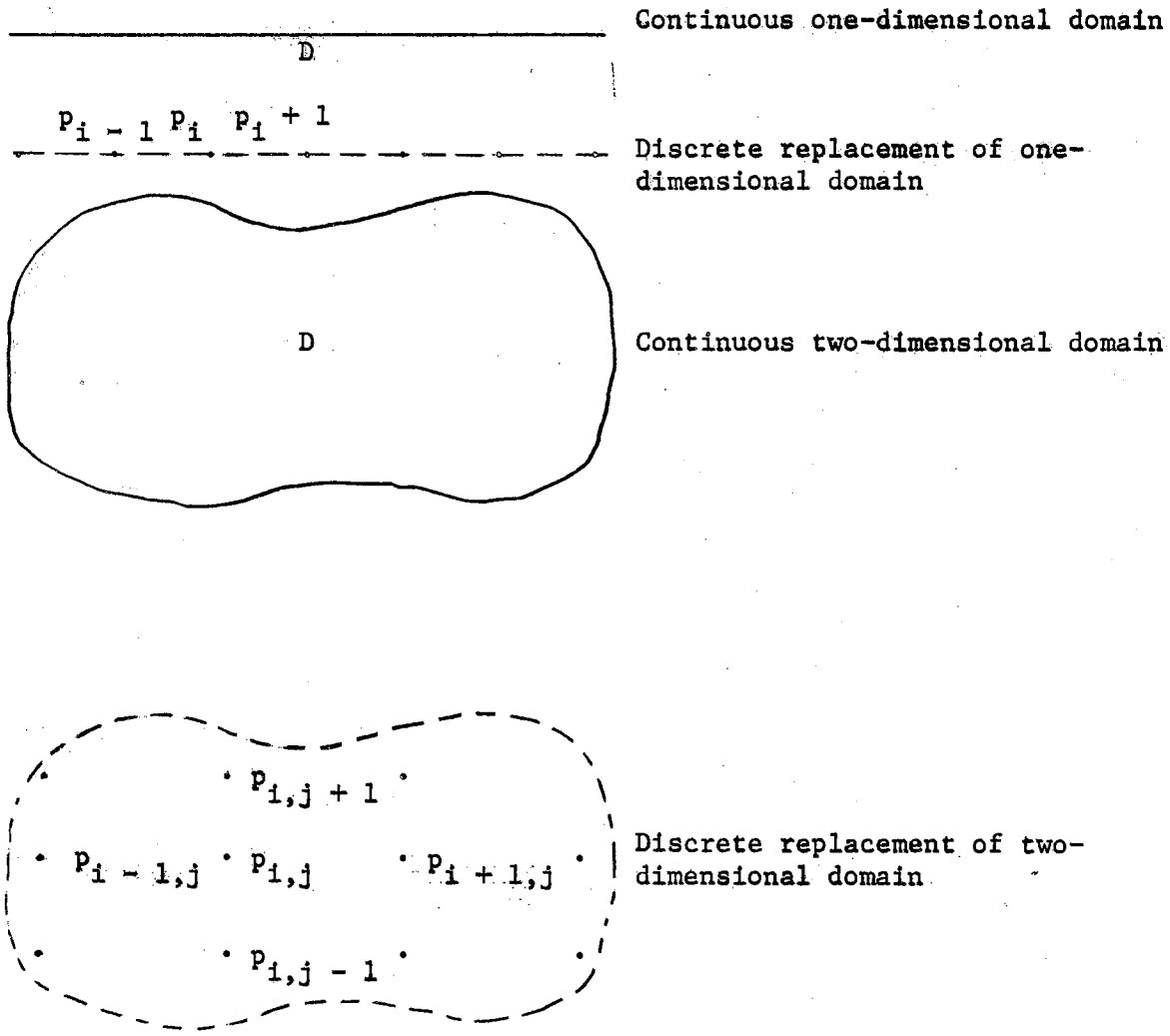

Figure 3. Approximation of a Continuous Domain by an Array of Discrete Points

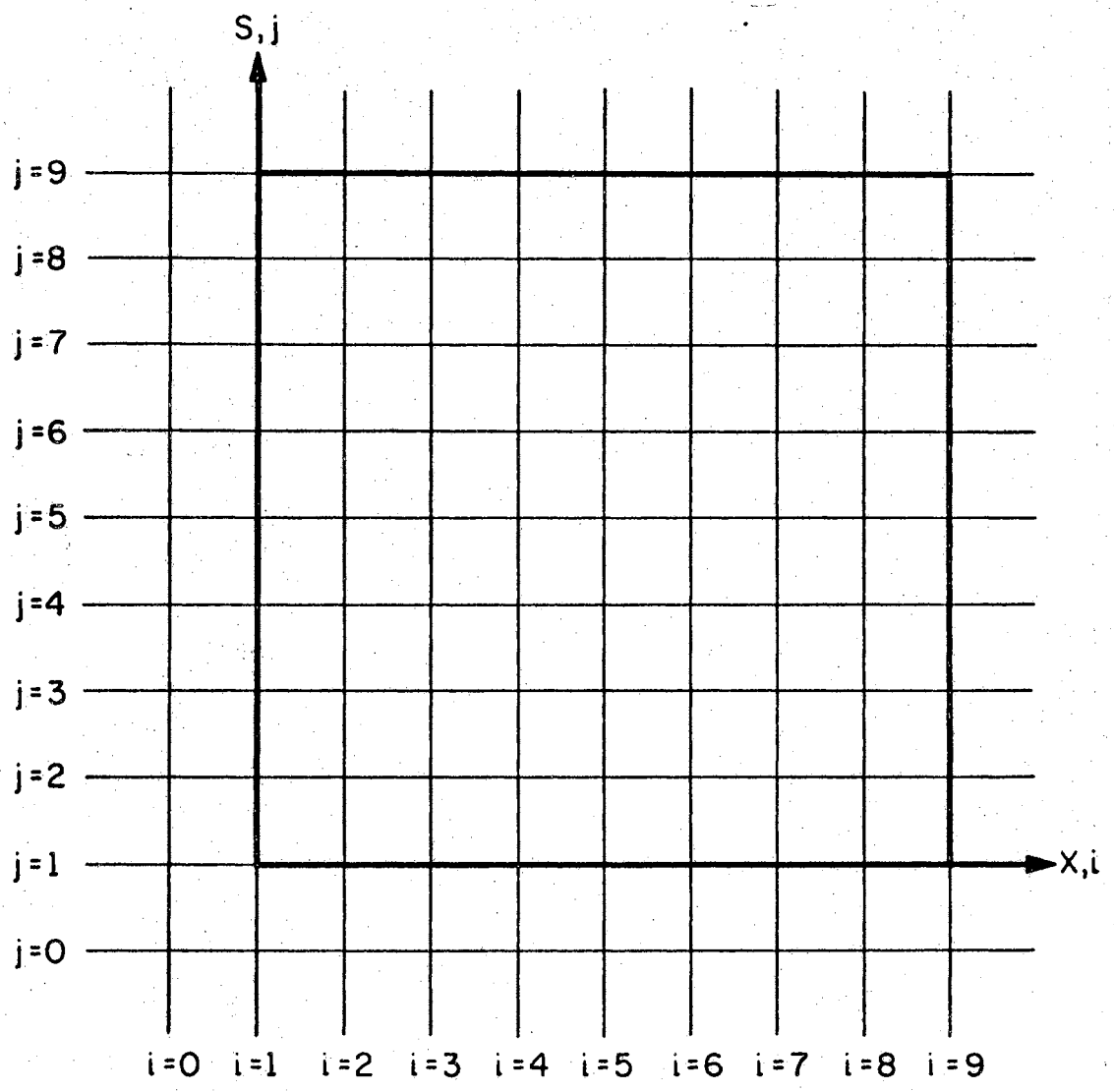

Figure 4. Grid System for Finite Difference Operators

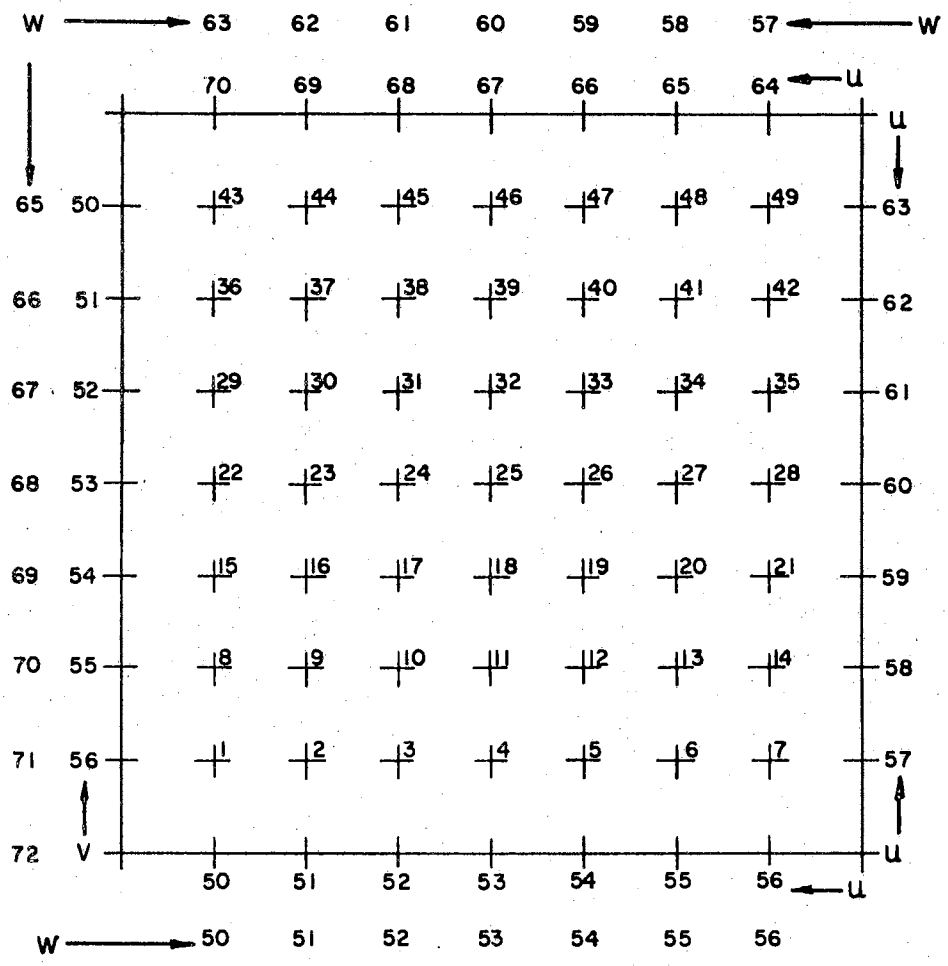

Figure 5. Numbering System for Variables

The points of application of the finite difference approximations for the closed shell are shown on a simplified grid system in Figure 6. The points of application for the open shell are shown in Figure 7.

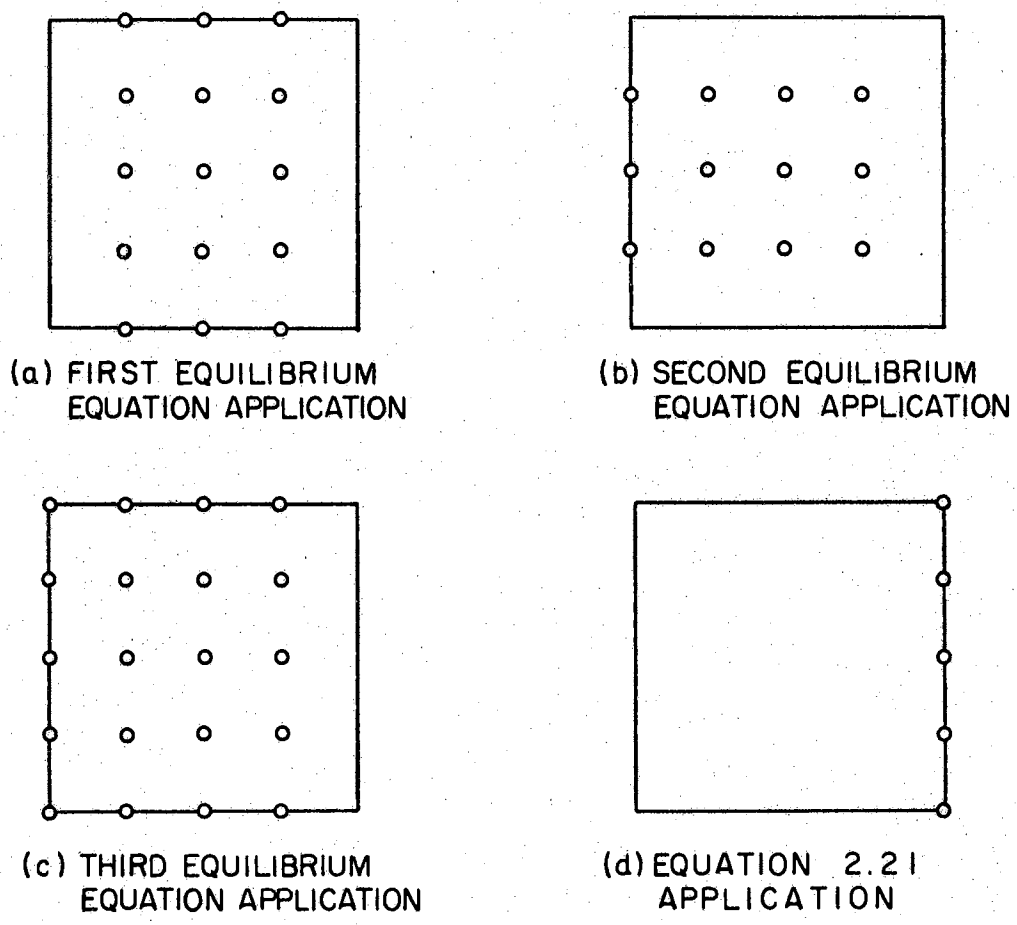

Figure 6. Points of Application of Finite Difference Approximations for Closed Shell

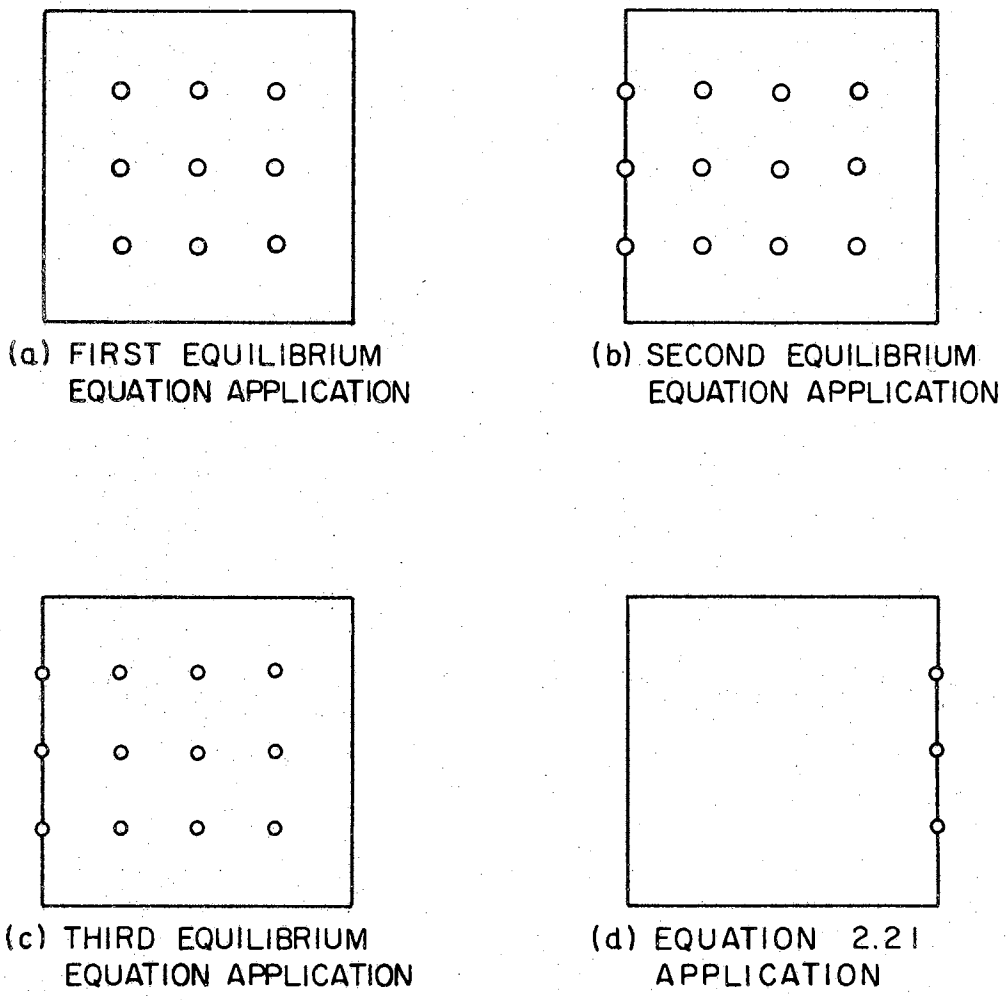

Figure 7. Points of Application of Finite Difference Approximations for an Open Shell

Using the concept of "fictitious points" (6) outside the boundary at $\zeta = 1$ and the conditions of symmetry on the other three sides of the

closed shell, the boundary conditions (Equations 2.14, 2.15, and 2.16) are expressed in terms of the finite difference approximations by Equations 2.18, 2.19, and 2.20 with the exception of $u,_{\zeta} = 0$ in Equation 2.16. Since the boundary at $\zeta = 1$ is allowed to translate, the condition $u,_{\zeta} = 0$ is expressed in terms of the backward difference expression (6) given by Equation 2.21.

$$\begin{aligned} u_{out} &= u_{in} \\ v_{out} &= -v_{in} \qquad \text{For } \eta = 0 \text{ and } \eta = 1 \text{ with } 0 \leq \zeta \leq 1 \\ w_{out} &= w_{in} \end{aligned} \tag{2.18}$$

$$\begin{aligned} u_{out} &= -u_{in} \\ v_{out} &= v_{in} \qquad \text{For } \zeta = 0 \text{ with } 0 \leq \eta \leq 1 \\ w_{out} &= w_{in} \end{aligned} \tag{2.19}$$

$$\begin{aligned} v_{out} &= v_{in} \\ w_{out} &= -w_{in} \end{aligned} \qquad \text{For } \zeta = 1 \text{ with } 0 \leq \eta \leq 1 \tag{2.20}$$

$$u,_{\zeta}\Big|_{i,j} = 0 = 3u_{i,j} - 4u_{i-1,j} + u_{i-2,j} \tag{2.21}$$

For the open shell Equations 2.19, 2.20, 2.21 were used for the boundaries of constant ζ. For boundaries of constant η; i.e., $\eta = 0$ and $\eta = 1$ with $0 \leq \zeta \leq 1$; the only condition required is

$$w_{out} = -w_{in} \tag{2.22}$$

CHAPTER III

COMPUTER SOLUTION

3.1 Coefficient Matrix

The differential equations which govern the deformation of a non-circular cylindrical shell are given by Equation 2.1. The equations are solved using the finite difference procedure as discussed in Chapter II. The equations together with the appropriate boundary conditions and conditions of symmetry are applied at the various grid points (Figure 4) to set up the relation between the deflections at these grid points and the loads applied at these grid points. This relation is given by Equation 3.1.

$$\{P\} = [A]\{\delta\} \tag{3.1}$$

where

$\{P\}$ = the grid point-forces

$\{\delta\}$ = the grid point-deflections

$[A]$ = the coefficient matrix relating the forces to the deflections.

Using the numbering system shown in Figure 5, the δ-matrix is ordered as shown in Equation 3.2. The coefficient matrix, A, in Equation 3.1 is obtained by applying the equilibrium equations at all interior points and at the appropriate boundary points and applying Equation 2.19 at points along the boundary at $\zeta = 1$, as shown in Equations 3.2.

$$
\begin{Bmatrix} \bar{P}_x \\ \bar{P}_s \\ \bar{P}_z \\ 0 \end{Bmatrix} =
\begin{bmatrix}
\text{First equilibrium equation applied at all interior points and at appropriate boundary points} \\
\text{Second equilibrium equation applied at all interior points and at appropriate boundary points} \\
\text{Third equilibrium equation applied at all interior points and at appropriate boundary points} \\
\text{Equation 2.21 applied along } \zeta = 1
\end{bmatrix}
\begin{Bmatrix}
u_1 \\ v_1 \\ w_1 \\ u_2 \\ v_2 \\ w_2 \\ \vdots \\ u_{48} \\ v_{48} \\ w_{48} \\ u_{49} \\ v_{49} \\ w_{49} \\ u_{50} \\ u_{51} \\ u_{52} \\ \vdots \\ u_{72} \\ v_{50} \\ v_{51} \\ v_{52} \\ \vdots \\ v_{56} \\ w_{50} \\ w_{51} \\ w_{52} \\ \vdots \\ w_{72}
\end{Bmatrix}
\tag{3.2}
$$

To eliminate numerical difficulties, some of the equations in the simultaneous set (Equation 3.2) were scaled in order that the terms of the coefficient matrix be of approximate equal magnitude. After the application of the equilibrium equations and the scaling operation was completed and the final form of the coefficient matrix was obtained,

the IBM scientific subroutine (8) SIMQ[1] was used to obtain the unknown deflections, $\{\delta\}$.

3.2 Computer Program

The computer program was organized to apply efficiently and methodically the finite difference form of the equilibrium equations. The program is separated into subroutines which supply the numerical value of each term of the coefficient matrix and a subroutine to store these values in the correct position in the matrix. The logic of the program is shown in the flow chart in Figure 8.

[1]SIMQ is a subroutine which obtains the solution of a set of simultaneous linear equations.

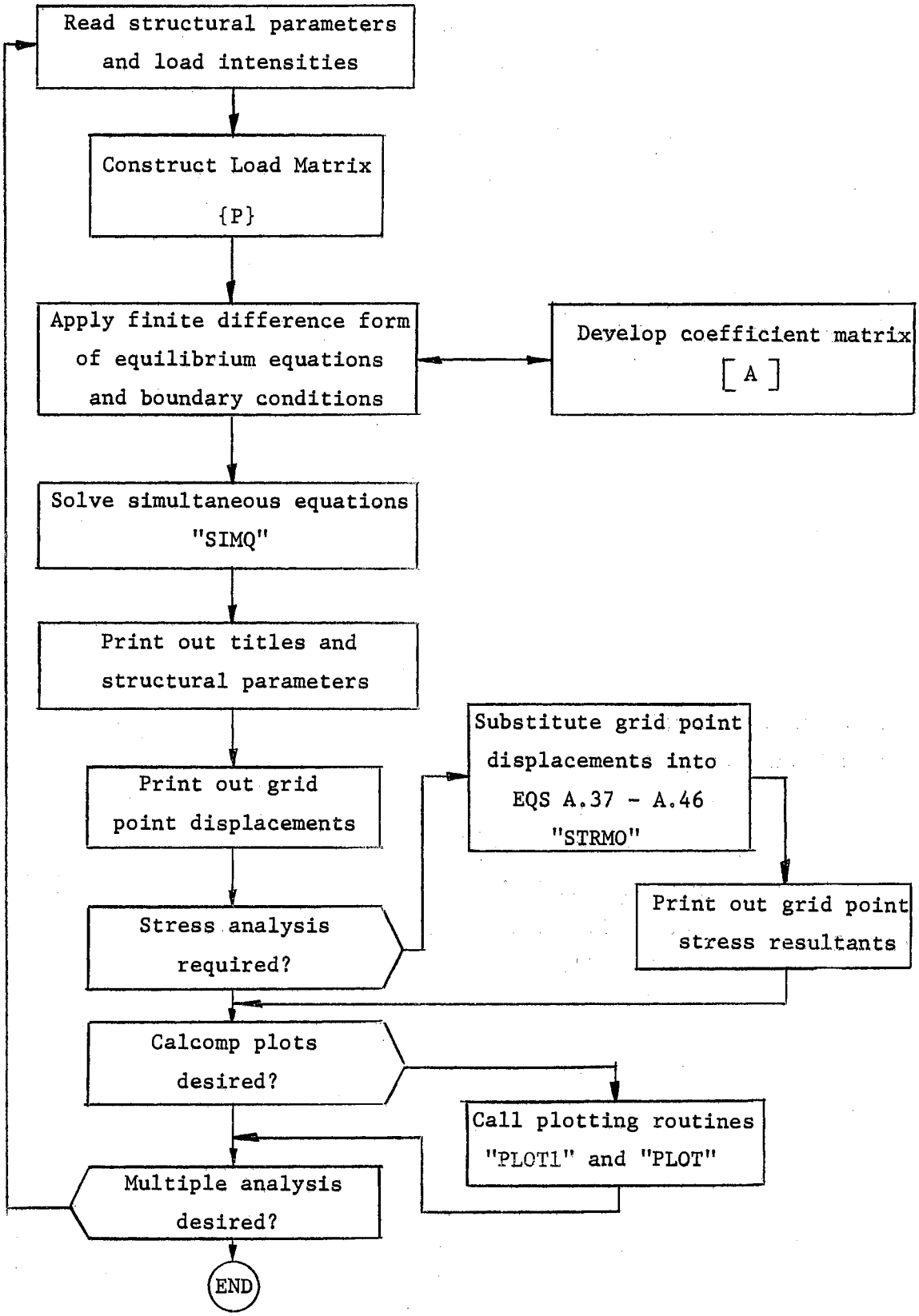

Figure 8. Computer Program Flow Chart

CHAPTER IV

NUMERICAL RESULTS

To check the validity of the formulation and the computer program several comparisons with existing solutions are made. Examples from References 4, 9, 10, and 11 are solved in this study and comparisons made in the following sections.

4.1 Comparison with Known Result for a Circular Cylindrical Shell

The basic boundary conditions discussed in Chapter II were modified so that a closed circular cylindrical shell with pinned ends could be analyzed. This circular cylindrical shell is acted upon by a uniform pressure loading and is shown in Figure 9. The axisymmetric shell with an axisymmetric load is almost a trivial case since the Donnell and Flugge equations are identical. However, to develop confidence in the method and the computer program, the analysis of closed circular cylinders was made and since the data was available, it is presented here for completeness. Timoshenko (9) gives as the magnitude of the radial deflection at the midpoint of the shell the relation in Equation 4.1.

$$w = \frac{PL^4}{64K\alpha^4}\left(1 - \frac{2\cos\alpha\cosh\alpha}{\cos 2\alpha + \cosh 2\alpha}\right) \qquad (4.1)$$

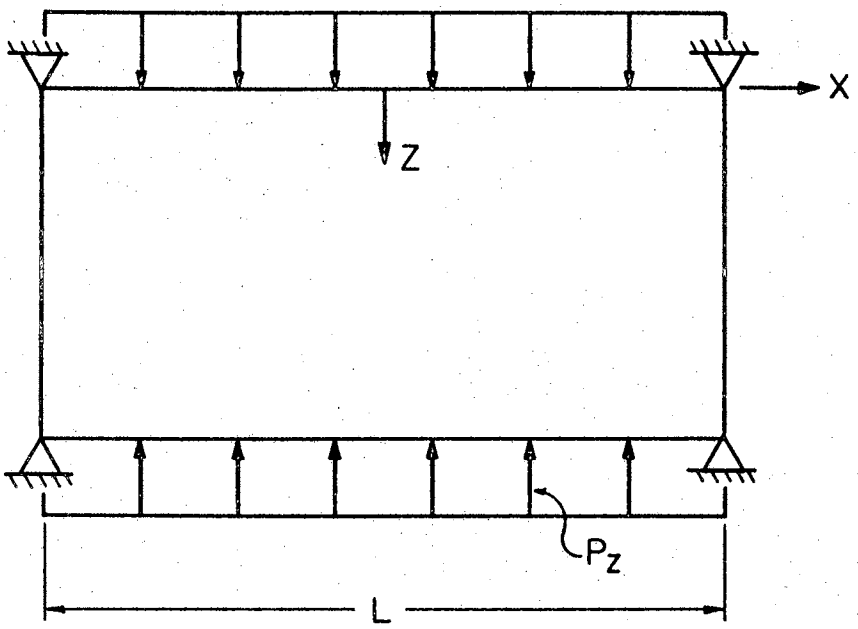

Figure 9. Pinned Supported Circular Cylinder With Uniform Pressure Load

where

P = intensity of the pressure loading

L = length of the shell

$\alpha = \frac{\beta L}{2}$

$\beta^4 = \frac{Eh}{4r^2K}$

h, r, and K are the same as used in this study (Chapter II). Comparisons between Equation 4.1 and numerical results are given by Table I.

For the case of open circular cylindrical shells, a simply supported cylindrical shell segment under uniform pressure p_z was considered. Comparison with the exact solution of the Donnell equations as given by Boyd (4) was made using both the Donnell and Flugge equations of the present study. The geometric properties of the shell considered as well as the results of the comparison are shown in Figure 10. The boundary conditions for this cylindrical shell segment are the same as those for open shells discussed in Section 2.4. For this example, the radial deflections, $\overline{w}$, are given in Table II for the solution of both the Donnell equations and the Flugge equations. In the case of this open shell segment under uniform pressure loading, the solutions given by the Donnell equations are in exact agreement with those given by the Flugge equations.

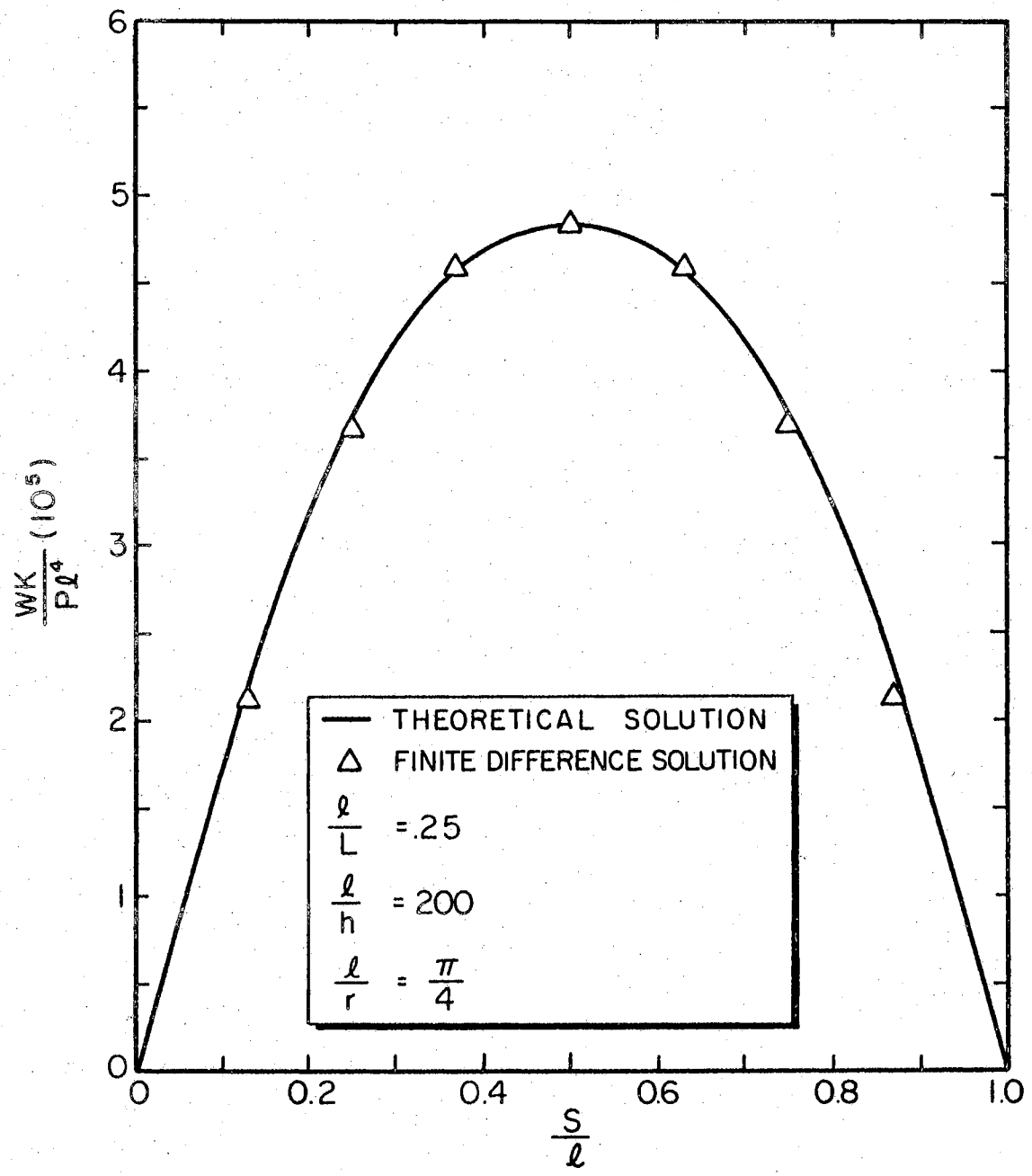

Figure 10. Radial Deflections for a Circular Shell Segment With Uniform Pressure Loading

TABLE I

RADIAL DEFLECTION AT MIDPOINT OF CIRCULAR CYLINDRICAL SHELL ACTED UPON BY A UNIFORM PRESSURE LOADING WITH $\frac{\ell}{h} = 200$

$\frac{\ell}{L}$	$\overline{w}$ - Theoretical	$\overline{w}$ - Numerical	% Error
0.1	1013.21	989.879	2
0.2	1013.21	989.879	2
0.3	1013.21	989.879	2
0.4	1013.21	989.880	2
0.5	1013.21	989.881	2
0.6	1013.21	989.883	2
0.7	1013.21	989.887	2
0.8	1013.21	989.893	2
0.9	1013.21	989.902	2
1.0	1013.21	989.914	2
2.0	1013.20	990.427	2
3.0	1012.95	992.367	2
4.0	1007.54	996.095	1
5.0	1016.51	1000.56	2
6.0	1049.26	1004.05	5
7.0	1090.80	1006.00	8

TABLE II

RADIAL DEFLECTIONS OF A CIRCULAR SHELL SEGMENT ACTED UPON BY A UNIFORM PRESSURE LOADING
$\frac{\ell}{r} = \frac{\pi}{4}$, $\frac{\ell}{L} = .25$, $\frac{\ell}{h} = 200$

$\frac{s}{\ell}$	$\bar{w}$ - Donnell	$\bar{w}$ - Flugge
0	0	0
.125	37463	37465
.250	64335	64338
.375	80356	80360
.500	85676	85680
.625	80356	80360
.750	64335	64338
.875	37463	37465
1.0	0	0

4.2 Comparison With Known Results for the Noncircular Cylindrical Shell

The short, slightly noncircular shell is well behaved and the solution is obtainable by several different analysis procedures. It is expected that all numerical methods of analysis based on the Kirchoff-Love assumptions should give good results for these shells. Two analyses, Romano (10) and Mah (11) were selected to establish the validity of the present method as applied to this type of shell. In the first example, Romano (10) used a Fourier series solution to obtain a solution of the Donnell equations for noncircular shells. Romano also obtained an approximate solution by solving the Donnell equations for a circular cylindrical shell using for the radius of the circular shell

the corresponding radius of the noncircular shell at the points of interest. This, of course, requires the solution of many circular cases in order to solve one noncircular case. The method was applied only to short shells.

The example problem solved by Romano (10) is a short, closed cylindrical shell with an oval cross section acted upon by a uniform pressure loading. The geometric properties and the radial deflections are given in Figure 11. The finite difference method of the present study compares very well with the solution given by Romano's exact method. As illustrated by Figure 11, the values of radial deflection along generators at $s/\ell = 0$, $s/\ell = 1/8$, and $s/\ell = 1/4$ from $x/L = 0$ to $x/L = 1$ are identical to Romano's exact solution. For this short shell, Table III compares the solutions given by the Donnell equations and by the Flugge equations. As expected, the Donnell equations compare faborably with the Flugge equations.

In the second example, Mah (11) uses a Fourier series to obtain a reduced set of differential equations, and then applies the finite difference method to obtain the solution of this reduced set of equations. Although the governing equations are equivalent in form to the Kempner form of the Flugge equations and should be applicable to long shell problems, Mah applies the solution procedure to short shells only. However, it should be pointed out that for long shells the series used converged much more slowly and a greater number of terms were required to perform the analysis. The present method, on the other hand, gives the solution for moderately long shells using the same basic setup as used for the short shells.

The sample problem selected for comparing the present method with

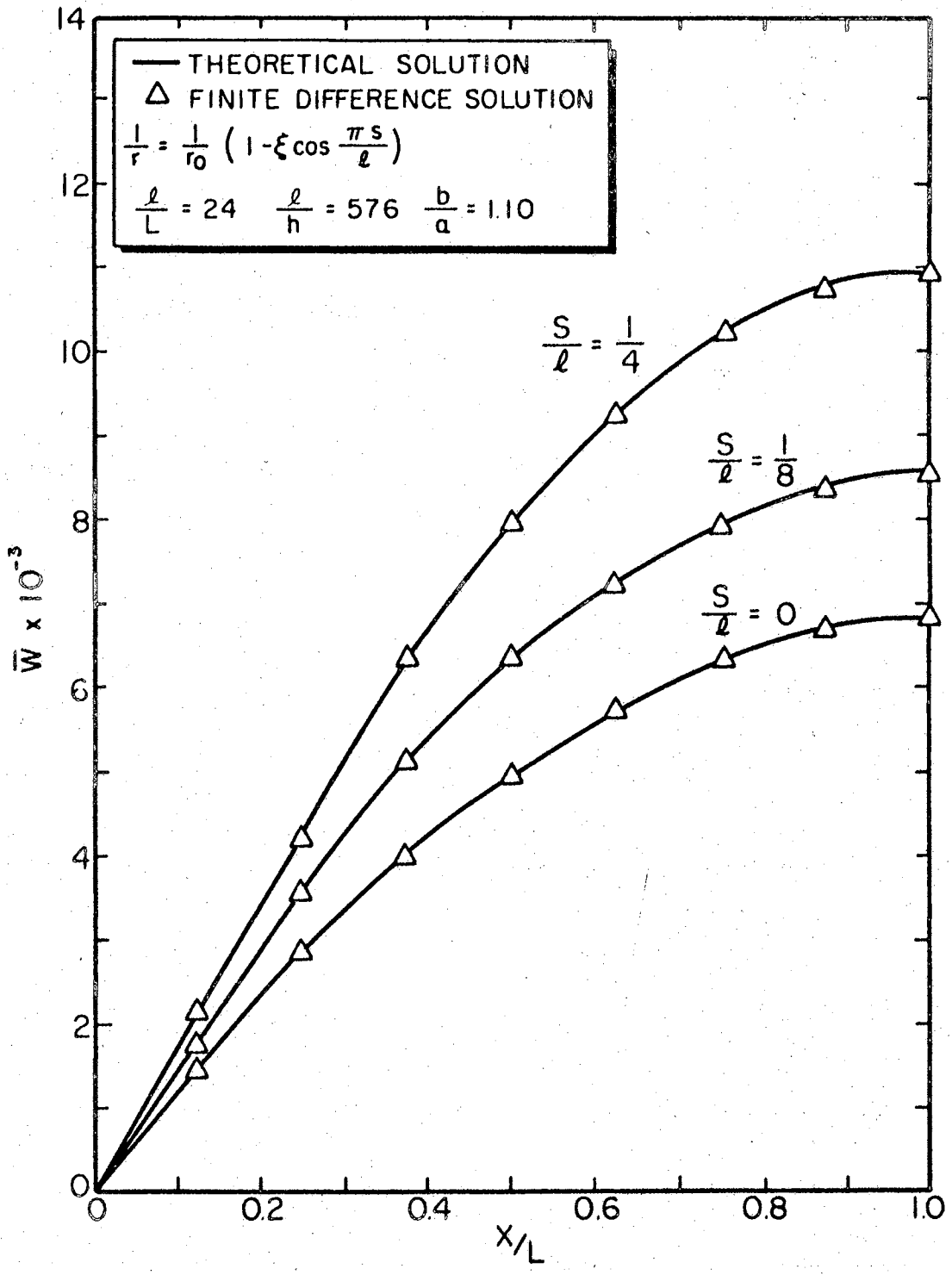

Figure 11. Radial Deflections for an Oval Cylindrical Shell With Uniform Pressure Load

TABLE III

RADIAL DEFLECTION COMPARISON FOR AN OVAL CYLINDER
$\frac{\ell}{h} = 576 \quad \frac{\ell}{L} = 24 \quad \frac{b}{a} = 1.10$

$\frac{x}{L}$	$\frac{s}{\ell} = 0$		$\frac{s}{\ell} = 1/8$		$\frac{s}{\ell} = 1/4$	
	$\bar{w}$ - Donnell	$\bar{w}$ - Flugge	$\bar{w}$ - Donnell	$\bar{w}$ - Flugge	$\bar{w}$ - Donnell	$\bar{w}$ - Flugge
0	6828	6790	8543	8494	10818	10758
.125	6720	6680	8402	8352	10634	10573
.250	6393	6350	7978	7927	10082	10019
.375	5843	5797	7272	7218	9167	9104
.500	5069	5022	6286	6233	7899	7838
.625	4072	4029	5029	4982	6298	6245
.750	2866	2834	3527	3490	4401	4361
.875	1487	1470	1824	1805	2270	2249
1.0	0	0	0	0	0	0

that of MAH is a closed cylindrical shell of elliptical cross section loaded by a uniform pressure. The geometric properties of this shell and the radial deflections are shown in Figure 12. The radial deflections of the shell along the curve at x/L = 0 for $s/\ell = 0$ to $s/\ell = 1/4$ using the finite difference method of the present study are also shown in Figure 12. As expected here also, agreement is good, with the maximum difference in the two solutions 4 percent. For this short shell, Table IV compares solutions given by the Donnell equations and by the Flugge equations. Here, too, good agreement is obtained.

TABLE IV

RADIAL DEFLECTION COMPARISON FOR AN ELLIPTICAL CYLINDER
$\frac{\ell}{h} = 763.7$ $\frac{\ell}{L} = 30.55$ $\frac{b}{a} = 1.413$

$4\frac{s}{\ell}$	$\bar{w}$ - Donnell	$\bar{w}$ - Flugge
0	45064	45012
.125	43238	43190
.250	37651	37615
.375	29970	29949
.500	21635	21628
.625	14281	14284
.750	8993	8999
.875	6061	6067
1.0	5221	5226

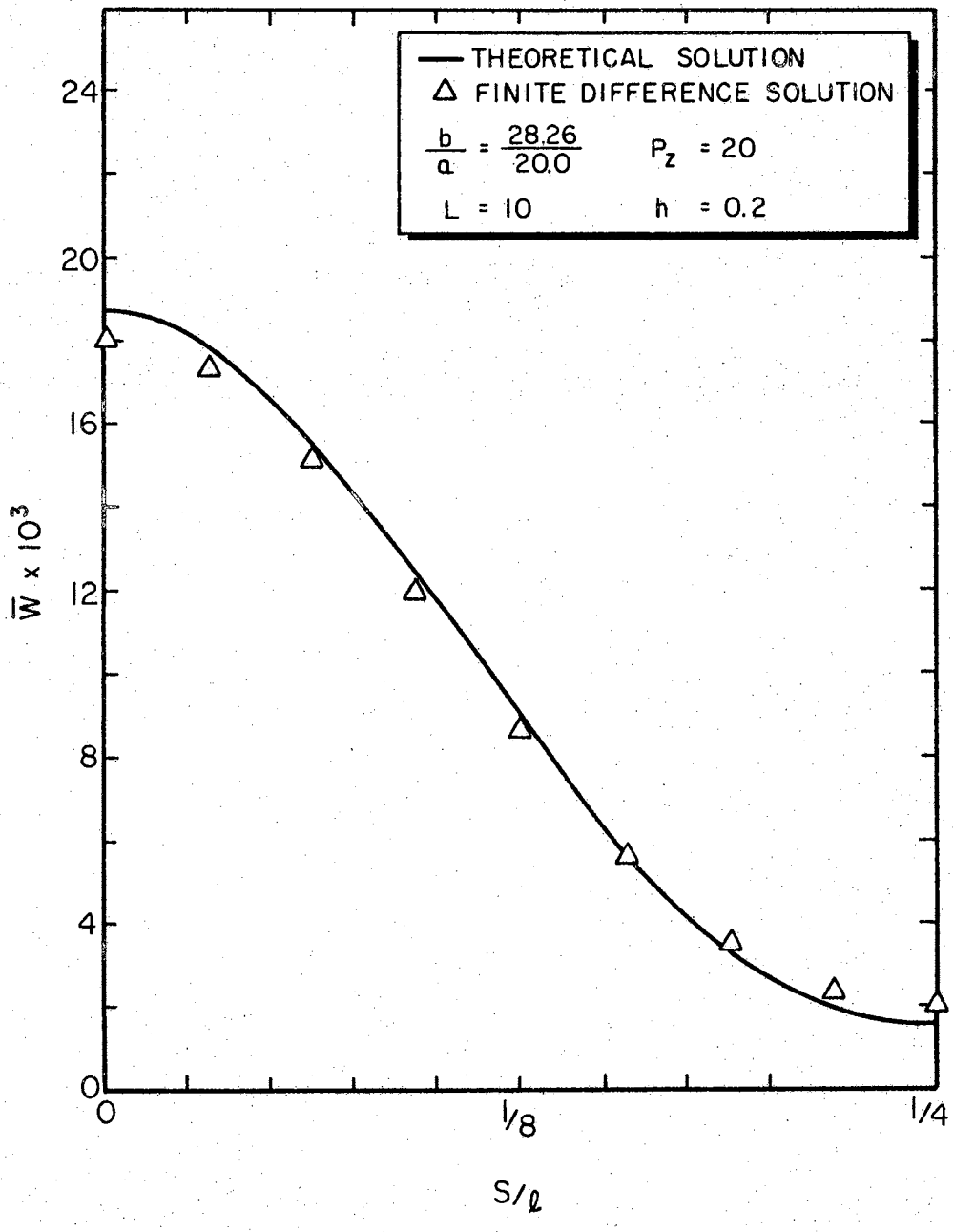

Figure 12. Radial Deflections for an Elliptical Cylindrical Shell With Uniform Pressure Loading

4.3 Accuracy of the Donnell Equations

The accuracy of the Donnell equilibrium equations (Equation 2.5) was established by comparing with numerical solutions to the Flugge equilibrium equations (Equation 2.1) using both a circular cylinder and an elliptical cylinder loaded along a generator as shown in Figure 13. The results of this comparison which are shown in Tables V and VI, are similar to those of Kraus (7). The present solution indicates the same characteristics, i.e., for the circular shell loaded along a generator the Donnell equations give unreliable results as the shell becomes longer and as the thickness approaches the lower limit of thinness. The noncircular cylinder exhibits the same characteristic. The results of this comparison are discussed in the next few paragraphs.

Corresponding to the tabulation by Kraus, Table V shows the comparison of the numerical solutions of the Donnell equations and the Flugge equations for a circular cylindrical shell. The radial deflection of point P ($s = 0$, $s = \frac{\ell}{4}$; Figure 13) is used as the basis for the comparison. The values of this radial deflection is tabulated for $\frac{\ell}{h}$ ratios of 50, 100, 200, 400, and 800; and for $\frac{\ell}{L}$ ratios of 10.0, 1.0, and 0.1. Inspection of this table shows that for very thin circular shells the finite difference solution of the Donnell equations is no different than the finite difference solution of the Flugge equations. As the thickness and the length of the shell is increased, the Donnell equations become more and more inaccurate. The greatest influence on this inaccuracy is felt to be the effect of the transverse shearing forces, Q_s acting on the thickness of the shell section. Obviously as the shell becomes thicker (but still a thin shell) the influence of the contribution of the transverse shear forces to the second equilibrium

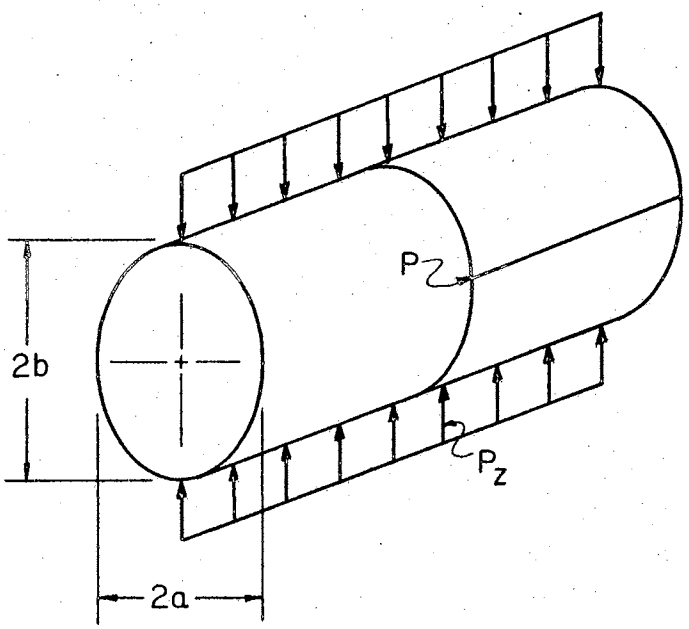

Figure 13. Elliptical Cylinder With Line Load

TABLE V

COMPARISON OF ACCURACY OF DONNELL EQUATIONS FOR CIRCULAR CYLINDRICAL SHELL WITH LOADING APPLIED TO GENERATORS

$\frac{\ell}{h}$	$\frac{\ell}{L}$	$\overline{w}_p$ - Donnell	$\overline{w}_p$ - Flugge
50	0.1	- 150.68	- 147.25
50	1.0	- 70.82	- 70.02
50	10.0	- 0.0013	- 0.0119
100	0.1	- 603.56	- 600.08
100	1.0	- 286.68	- 285.85
100	10.0	- 0.106	- 0.110
200	0.1	-2415.1	-2411.6
200	1.0	-1150.0	-1149.2
200	10.0	0.105	0.100
400	0.1	-9661.2	-9657.7
400	1.0	-4603.4	-4602.6
400	10.0	- 0.627	- 0.634
800	0.1	-38645.7	-38642.2
800	1.0	-18417.0	-18416.1
800	10.0	- 3.553	- 3.561

TABLE VI

COMPARISON OF ACCURACY OF DONNELL EQUATIONS FOR ELLIPTICAL CYLINDRICAL SHELL WITH LOADING APPLIED TO GENERATORS

		$\frac{b}{a} = 5$		$\frac{b}{a} = 10$	
$\frac{\ell}{h}$	$\frac{\ell}{L}$	$\bar{w}_p$ - Donnell	$\bar{w}_p$ - Flugge	$\bar{w}_p$ - Donnell	$\bar{w}_p$ - Flugge
50	0.1	- 55.77	- 18.888	- 21.978	- 0.499
50	1.0	- 20.332	- 8.954	- 6.133	- 0.228
50	10.0	- 0.0365	- 0.0390	- 0.0047	- 0.0040
100	0.1	- 244.579	- 161.794	- 115.12	- 11.67
100	1.0	- 105.698	- 79.148	- 41.69	- 6.271
100	10.0	- 0.380	- 0.353	- 0.114	- 0.0523
200	0.1	- 1004.19	- 889.02	- 507.17	- 160.66
200	1.0	- 465.25	- 428.65	- 218.38	- 90.75
200	10.0	- 0.639	- 0.620	- 0.808	- 0.559
400	0.1	- 4044.09	- 3916.82	-2085.6	-1357.5
400	1.0	- 1913.20	- 1873.03	- 965.04	- 712.97
400	10.0	+ 0.700	+ 0.698	- 1.379	- 1.229
800	0.1	-16204.1	-16073.4	-8402.8	-7410.24
800	1.0	- 7708.24	- 7667.08	-3973.83	-3650.38
800	10.0	+ 1.259	+ 1.256	1.415	1.376

equation (Equation A.2) becomes greater and should not be neglected.

To illustrate the effect of noncircularity on the accuracy of the Donnell equations, an elliptical cylindrical shell loaded by a line load (Figure 13) is analyzed. The radial deflection of point P given by this analysis is tabulated (Table VI) for $\frac{b}{a}$ ratios of 5 and 10; and for $\frac{\ell}{h}$ ratios of 50, 100, 200, 400, and 800, and for $\frac{\ell}{L}$ ratios of 10.0, 1.0, and 0.1. A similar comparison to further illustrate the effect of noncircularity on the accuracy of the Donnell equations is shown in Tables VII, VIII, and IX. Here the radial deflection of point P for the elliptical cylindrical shell of Figure 13 is tabulated for $\frac{b}{a}$ ratios of 1 to 10 for three $\frac{\ell}{h}$ ratios (100, 200, and 400) for the single nondimensional length of 0.1. Also shown in these tables is the percent error of the Donnell equations with respect to the Flugge equations. Inspection of these tables shows that the noncircularity of the section plays an important role in the accuracy of the Donnell equations.

In order to establish limits for the use of the Donnell equations one final comparison is made. Figure 14 shows the radial deflection comparison for the elliptical cylindrical shell as a function of $\frac{\ell}{L}$. Inspection of the figure shows that for a ratio of $\frac{\ell}{h} = 50$ the $\frac{\ell}{L}$ value of 8 should be the limiting value for the use of the Donnell equations for $\frac{b}{a} = 5$. From Figure 15 the corresponding limits for $\frac{\ell}{h} = 100$ are $\frac{\ell}{L} = 8$ for $\frac{b}{a} = 5$ and $\frac{\ell}{L} = 15$ for $\frac{b}{a} = 10$. The finite difference method provided no significant information for a limit for the circular shell.

TABLE VII

RADIAL DEFLECTION COMPARISON FOR AN ELLIPTICAL CYLINDER WITH $\frac{\ell}{L} = 0.1$ and $\frac{\ell}{h} = 100$

$\frac{b}{a}$	$\overline{w}_p$ - Donnell	$\overline{w}_p$ - Flugge	% Error
1	-603.56	-600.08	1/2
2	-501.34	-498.87	1/2
3	-383.46	-374.33	2
4	-301.29	-258.54	17
5	-244.58	-161.79	51
6	-203.65	- 96.44	111
7	-173.19	- 56.30	207
8	-149.45	- 32.63	360
9	-130.50	- 19.30	580
10	-115.12	- 11.67	890

TABLE VIII

RADIAL DEFLECTION COMPARISON FOR AN ELLIPTICAL CYLINDER WITH $\frac{\ell}{L} = 0.1$ AND $\frac{\ell}{h} = 200$

$\frac{b}{a}$	$\overline{w}_p$ - Donnell	$\overline{w}_p$ - Flugge	% Error
1	-2415.09	-2411.59	-
2	-2011.26	-2008.76	-
3	-1547.05	-1537.49	1
4	-1225.12	-1175.67	4
5	-1004.19	- 889.02	13
6	- 846.10	- 660.76	28
7	- 728.66	- 478.86	52
8	- 637.90	- 337.24	90
9	- 565.73	- 233.70	144
10	- 507.17	- 160.66	280

TABLE IX

RADIAL DEFLECTION COMPARISON FOR AN ELLIPTICAL CYLINDER WITH $\frac{\ell}{L} = 0.1$ AND $\frac{\ell}{h} = 400$

$\frac{b}{a}$	$\overline{w}_p$ - Donnell	$\overline{w}_p$ - Flugge	% Error
1	-9661.20	-9657.7	-
2	-8051.0	-8048.5	-
3	-6201.69	-6192.01	-
4	-4921.21	-4869.78	1
5	-4044.09	-3916.82	3
6	-3418.58	-3194.05	7
7	-2954.41	-2613.09	13
8	-2597.28	-2124.05	22
9	-2314.54	-1708.99	35
10	-2085.60	-1357.45	54

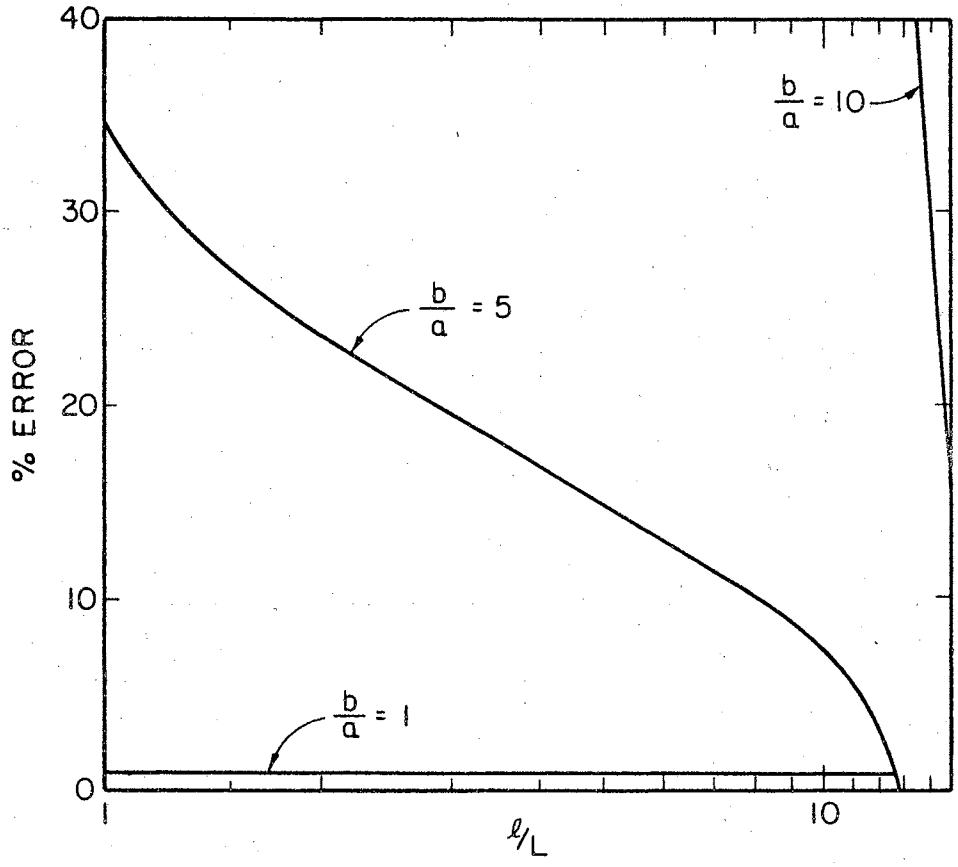

Figure 14. Radial Deflection Comparison for an Elliptical Cylinder with $\frac{\ell}{h} = 50$

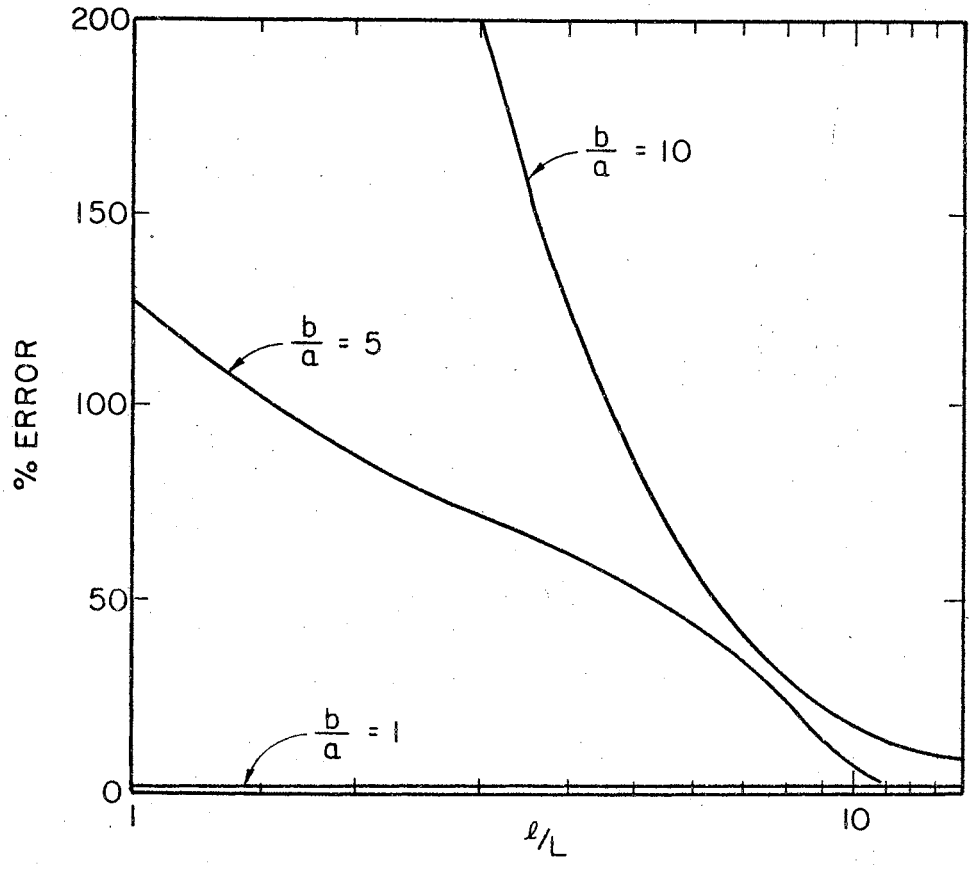

Figure 15. Radial Deflection Comparison for an Elliptical Cylinder with $\frac{\ell}{h} = 100$

CHAPTER V

SUMMARY AND CONCLUSIONS

5.1 Summary

A method has been presented to determine the deformation of a general noncircular cylindrical shell, either open or closed, using the Flugge equations of equilibrium. A special case of a general noncircular shell is the circular shell. From this study the following observations were made:

1. Through comparison of deflections obtained by other methods for identical noncircular shells, the finite difference method of analysis was shown to give valid results for the solution of the partial differential equations for noncircular shells.

2. For short noncircular shells the Donnell equilibrium equations compare favorably with the more accurate Flugge equilibrium equations.

3. For noncircular shells with axisymmetric loads the finite difference method does not indicate any significant inaccuracy of the Donnell equations as compared with the Flugge equations.

4. For a fixed shell cross section, properties, and loading, the accuracy of the Donnell equations was found to be adversely affected by an increase in the thickness of the shell.

5. For a fixed shell thickness, length, and loading, the accuracy of the Donnell equations was found to be adversely affected by an increase in the noncircularity of the shell crosssection.

6. For a fixed shell thickness, cross section, and loading, the accuracy of the Donnell equations was found to be adversely affected by an increase in the length of the shell.

7. The tabulation of the accuracy of the Donnell equations with respect to the Flugge equations fulfills a much needed comparison heretofore not published in the literature (7).

5.2 Conclusions

The calculation of the deformation of noncircular cylindrical shells using the more accurate Flugge equations was possible using this method. The method provides engineers with a tool for applying these more accurate equations. It also provides a basis for extending the more accurate equations to the dynamic and stability analyses of noncircular cylindrical shells. This study indicates a limiting value of $\frac{\ell}{L}$ for the application of the Donnell equations to noncircular shells loaded along a generator. The study points up the fact that the accuracy of the Donnell equations is sensitive to increasing shell thicknesses, the length of the shell, and the noncircularity of the cross section. The study also indicates that of these three, the thickness has the most effect on the accuracy of the Donnell equations.

5.3 Suggestions for Further Work

During this study, many interesting topics were noted which should be studied. In the finite difference method of solving the partial differential equations it is recognized that the grid spacing used in this study is not accurate for very long shells. A study should be made to improve the accuracy of the method for long shells. This could

be done by using a variable instead of a constant grid spacing. Further study in this area may: 1) incorporate higher order finite difference quotients; 2) evaluate and optimize a grid size as a function of the length of the shell.

Additional properties of the shell should be incorporated into this theory. For example, when applying the method to the analysis of shell structures for aircraft, including helicopters, submarines, and space vehicles it would be desirable to incorporate anisotropic material properties as well as variable thicknesses. In order for the investigation of noncircular cylindrical shells to be complete, studies should be made to determine the dynamic and stability characteristics of long shells. Also it would be desirable to obtain experimental verification of the deformations obtained in this study.

BIBLIOGRAPHY

(1) Kempner, Joseph, "Energy Expressions and Differential Equations for Stress and Displacement Analyses of Arbitrary Cylindrical Shells," Jour. of Ship Res., June 1958, pp. 8-19.

(2) Flugge, W., Stresses in Shells. Springer-Verlag Inc., New York, 1966.

(3) Donnell, L. H., "Stability of Thin-Walled Tubes Under Torsion," NACA Rep. No. 479, 1934.

(4) Boyd, D. E., "Analysis of Open Noncircular Cylindrical Shells," AIAA, Vol. 7, No. 3, 1969.

(5) McCracken, D. D. and Dorn, W. S., "Numerical Methods and Fortran Programming," John Wiley and Sons, Inc., New York, 1967.

(6) Salvadori, Mario G. and Baron, Melvin L., "Numerical Methods in Engineering," Prentice-Hall, Inc., Englewood Cliffs, New Jersey, 1952.

(7) Kraus, H., Thin Elastic Shells. John Wiley and Sons, Inc., New York, 1967.

(8) IBM Application Program H20-0205-2, "System/360 Scientific Subroutine Package (360A - CM - 03X) Version II Programmer's Manual," International Business Machines Corp., White Plains, New York, 1966.

(9) Timoshenko, S. and Krieger, S. Woinonsky, "Theory of Plates and Shells," Second Edition, McGraw-Hill Book Col, Inc., New York, 1959.

(10) Romano, Frank and Kempner, Joseph, "Stresses in Short Noncircular Cylindrical Shells Under Lateral Pressure," Journal of Applied Mechanics, Dec. 1962, p. 669-674.

(11) Mah, Gordon B. J., "Numerical Analysis of Noncircular Cylindrical Shells," Journal of the Engineering Mechanics Division, Proceedings of the American Society of Civil Engineers, June 1967, p. 219-237.

APPENDIX A

DERIVATION OF PARTIAL DIFFERENTIAL EQUATIONS OF EQUILIBRIUM (1)

A.1 Assumptions

In the derivation of the partial differential equations which give the deformations u, v, and w of the shell, the following assumptions are made:

1. The shell is cylindrical, i.e., its cross section is characterized by the plane curve resulting from the intersection of the median surface and a plane normal to the axis of the cylinder.

2. The right-handed coordinate system shown in Figure 16 gives the coordinates of any point (x, s, z) in the wall of the shell.

3. The material of the shell is isotropic, homogeneous and elastic.

4. The thickness of the shell is very small compared to the other dimensions of the shell.

5. The deformations u, v, and w are small compared to the thickness of the shell and do not significantly change the geometry of the shell.

6. The Kirchoff-Love assumptions of thin walled shell theory are applied; i.e., normals to the median surface of the undeformed shell remain straight, unextended, and normal to the median surface after deformation.

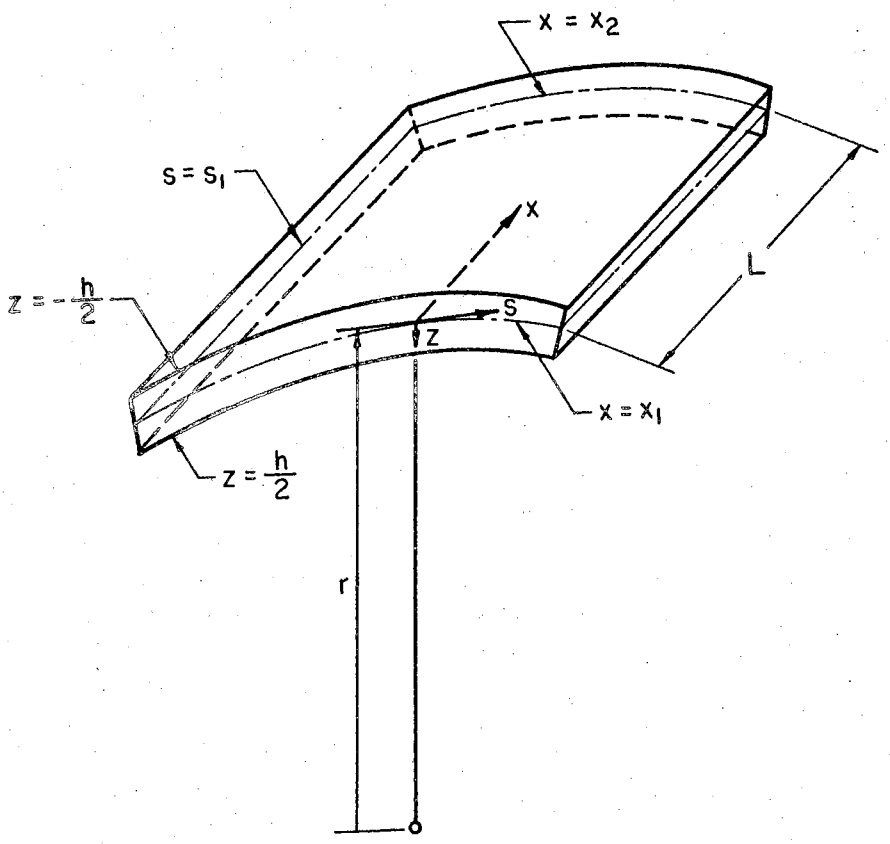

Figure 16. Sign Convention for Coordinates

7. The loading is applied at the median surface.

8. The stresses at any point in the shell wall are related to the strains through Hooke's Law for plane stress.

A.2 Equilibrium of Stress Resultants

Referring to Figures 17 and 18, equilibrium of forces in the x, s, and z directions and equilibrium of moments about these axes leads to the following six equations:[1]

$$N_{x,_x} + N_{sx,_s} = - P_x \tag{A.1}$$

$$N_{s,_s} + N_{sx,_x} - \frac{Q_s}{r} = - P_s \tag{A.2}$$

$$Q_{x,_x} + Q_{s,_s} + \frac{N_s}{r} = - P_z \tag{A.3}$$

$$M_{s,_s} + M_{xs,_x} - Q_s = 0 \tag{A.4}$$

$$M_{x,_x} + M_{sx,_s} - Q_x = 0 \tag{A.5}$$

$$N_{xs} - N_{sx} - \frac{M_{sx}}{r} = 0 \tag{A.6}$$

in which the stress resultants N (membrane) and M (bending or twisting) are related to the axial, circumferential, and shear stresses σ_x, σ_y, and τ_{xy} (= τ_{yx}) at any distance z from the median surface (Figure 19)

---

[1]Notation is given in Chapter II and not recorded here.

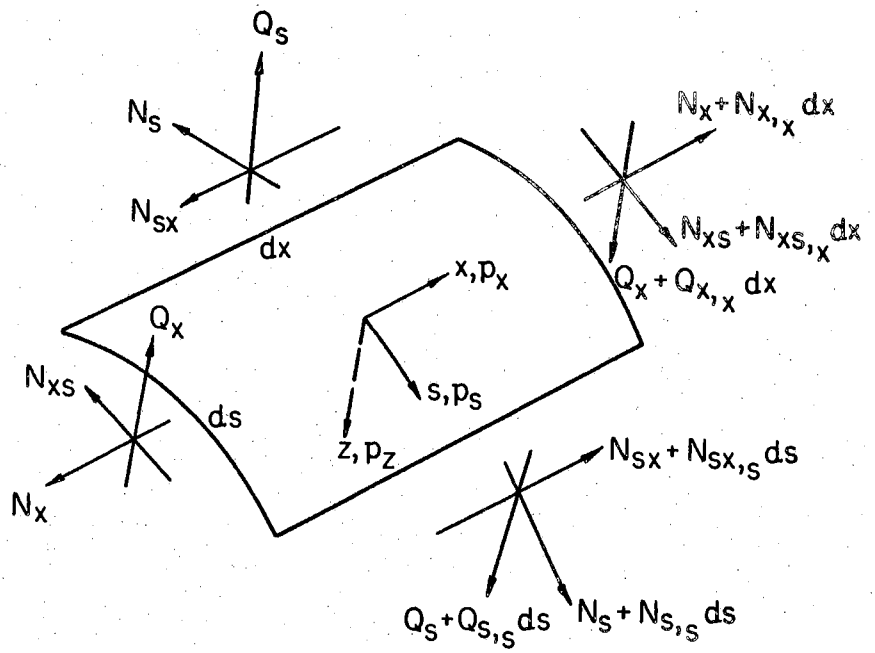

Figure 17. Sign Convention for Membrane and Transverse Shear Force Resultants and Loads

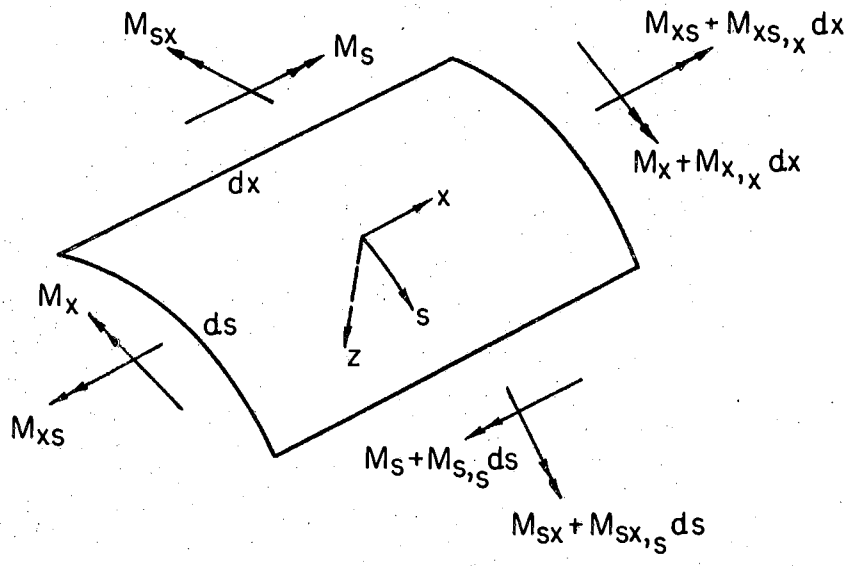

Figure 18. Sign Convention for Bending and Twisting Moment Resultants

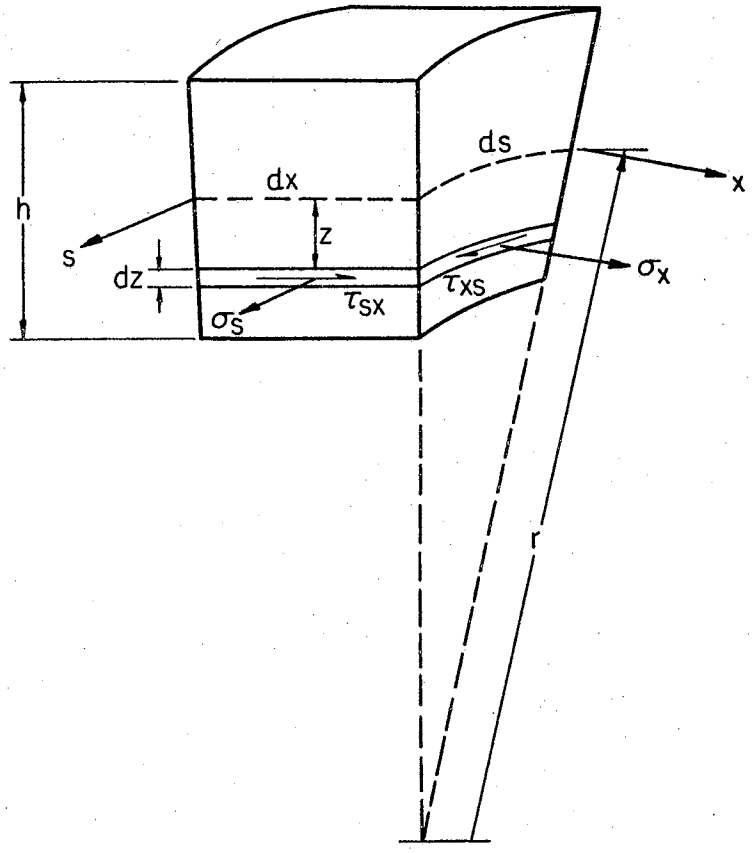

Figure 19. Sign Convention for Stresses on the Element

by the following relations:

$$N_x = \int_{-1/2\ h}^{1/2\ h} \sigma_x \left(1 - \frac{z}{r}\right) dz \tag{A.7}$$

$$N_{xs} = \int_{-1/2\ h}^{1/2\ h} \tau_{xs} \left(1 - \frac{z}{r}\right) dz \tag{A.8}$$

$$N_{sx} = \int_{-1/2\ h}^{1/2\ h} \tau_{sx}\, dz \tag{A.9}$$

$$N_s = \int_{-1/2\ h}^{1/2\ h} \sigma_s\, dz \tag{A.10}$$

$$M_x = \int_{-1/2\ h}^{1/2\ h} \sigma_x \left(1 - \frac{z}{r}\right) z dz \tag{A.11}$$

$$M_{xs} = -\int_{-1/2\ h}^{1/2\ h} \tau_{xs} \left(1 - \frac{z}{r}\right) z dz \tag{A.12}$$

$$M_{sx} = \int_{-1/2\ h}^{1/2\ h} \tau_{sx}\, z dz \tag{A.13}$$

$$M_s = \int_{-1/2\ h}^{1/2\ h} \sigma_s\, z dz \tag{A.14}$$

From Equations A.4 and A.5 the transverse shear resultants are defined by Equations A.15 and A.16.

$$Q_x = M_{x,_x} + M_{sx,_s} \tag{A.15}$$

$$Q_s = M_{s,_s} - M_{xs,_x} \tag{A.16}$$

Note: Equation A.6 is identically satisfied when Equations A.8, A.9, and A.12 are substituted therein.

The three equilibrium equations in terms of the stress resultants are obtained by substituting Equations A.15 and A.16 into Equations A.2 and A.3. Thus

$$N_{x,_x} + N_{xs,_s} = - P_x \tag{A.1}$$

$$N_{s,_s} + N_{xs,_x} - \left(\frac{M_{s,_s}}{r} + \frac{M_{xs,_x}}{r} \right) = - P_s \tag{A.17}$$

$$M_{x,_{xx}} + M_{s,_{ss}} + (M_{sx} - M_{xs})_{,_{xs}} + \frac{N_s}{r} = - P_z \tag{A.18}$$

Note: Up to this point in the derivation, the equations are identical in form to the corresponding equations for circular cylindrical shells (see, for example, Reference 2).

A.3 Strain-Displacement Relations

With assumptions 5 and 6 the axial, circumferential, and radial displacements at any point in the shell wall, u_z, v_z, and w_z, respectively, can be expressed in terms of the corresponding median surface displacements u(x, s), v(x, s), and w(x, s) as well as the axial and circumferential components of rotation of the normal at the median surface ω_x and ω_s, respectively. From Figures 20 and 21.

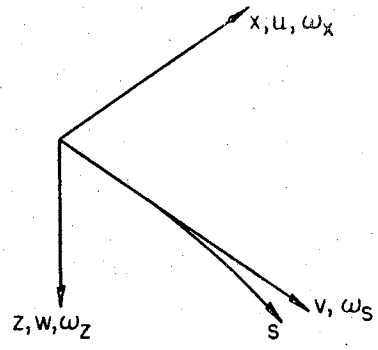

Figure 20. Sign Convention for Displacements and Rotations

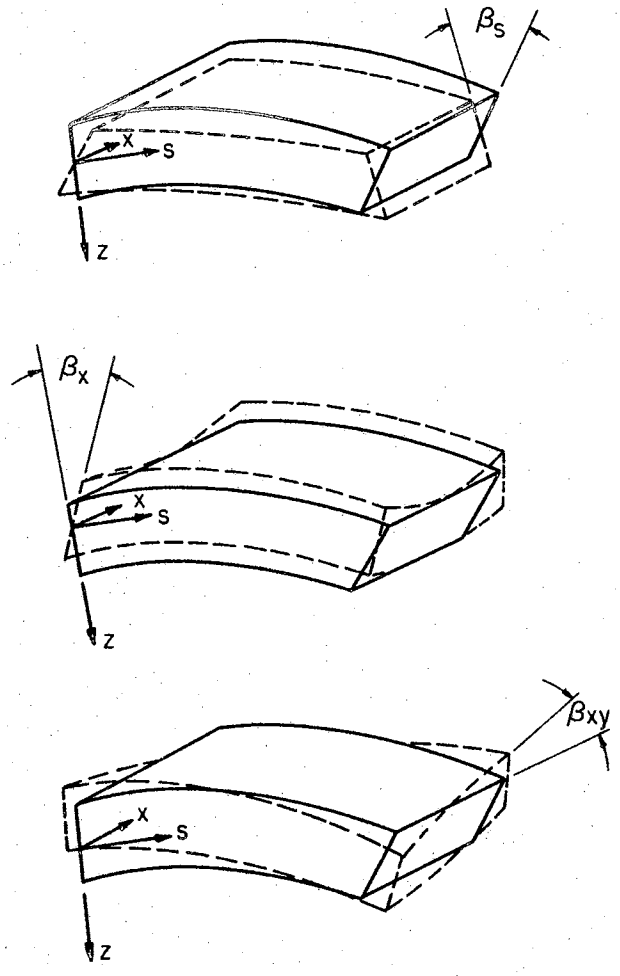

Figure 21. Element Deformation

$$u_z = u + z\omega_s \tag{A.19}$$

$$v_z = v - z\omega_x \tag{A.20}$$

$$w_z = w \tag{A.21}$$

where

$$\omega_x = w,_s + \frac{v}{r} \tag{A.22}$$

$$\omega_s = - w,_x \tag{A.23}$$

and

$$\omega_{x,_x} = - \omega_{s,_s} + \frac{v,_x}{r} \quad . \tag{A.24}$$

The strains at any point in the shell wall are related to the corresponding displacements by means of the well-known strain displacement relations expressed in cylindrical coordinates. Hence,

$$\varepsilon_x = u_{z,_x} \tag{A.25}$$

$$\varepsilon_s = \frac{1}{1 - \frac{z}{r}} \left[v_{z,_s} - \frac{w_z}{r} \right] \tag{A.26}$$

$$\varepsilon_{xs} = \varepsilon_{sx} = v_{z,_x} + \frac{1}{1 - \frac{z}{r}} u_{z,_s} \tag{A.27}$$

in which ε_x, ε_y, ε_{xy}, respectively, are the axial, circumferential, and shearing strains describing the state of strain in any plane tangential

to the cylindrical surface r(s), z . In terms of the displacement and rotation components of the median surface, the strain displacement relations become:[1]

$$\varepsilon_x = u,_x + z\omega_{s,_x} \tag{A.28}$$

$$\varepsilon_s = \frac{1}{1 - \frac{z}{r}} \left[v,_s - \frac{w}{r} - z\omega_{x,_s} \right] \tag{A.29}$$

$$\varepsilon_{xs} = \frac{1}{1 - \frac{z}{r}} u,_s + v,_x + \frac{z}{1 - \frac{z}{r}} \omega_{s,_s} - z\omega_{x,_x} \tag{A.30}$$

In terms of the corresponding median surface displacements and their derivatives the strains are:

$$\varepsilon_x = u,_x - zw,_{xx} \tag{A.31}$$

$$\varepsilon_s = \frac{1}{1 - \frac{z}{r}} \left\{ \left[(1 - \frac{z}{r})\, v \right]_{,_s} - zw,_{ss} + \frac{w}{r} \right\} \tag{A.32}$$

$$\varepsilon_{xs} = \frac{1}{1 - \frac{z}{r}} u,_s + (1 - \frac{z}{r})\, v,_x - \left[1 + \frac{1}{1 - \frac{z}{r}} \right] zw,_{xs} \tag{A.33}$$

A.4 Stress Resultants in Terms of Displacements

The stresses at any point in the shall wall are related to the strains through Hooke's law for plane stress.

---

[1]Physical interpretation and notation change of the $\omega_{s,_x}$ and $\omega_{x,_s}$ and $\omega_{x,_x}$ are available in many references. See, for example, Reference 2.

$$\sigma_x = \frac{E}{1-\nu^2}(\varepsilon_x + \nu\varepsilon_s) \tag{A.34}$$

$$\sigma_s = \frac{E}{1-\nu^2}(\varepsilon_s + \nu\varepsilon_x) \tag{A.35}$$

$$\tau_{xs} = \tau_{sx} = \frac{E}{2(1+\nu)}\varepsilon_{xs} \tag{A.36}$$

in which E is Young's modulus and ν is Poisson's ratio. Substitution of these stresses into Equations A.7 through A.14 and integrating yield expressions for the stress resultants in terms of the median surface displacements, Equations A.37 through A.44.

$$N_x = D\left[u_{,x} + \nu v_{,s} - \nu\frac{w}{r}\right] + K\left[\frac{1}{r}w_{,xx}\right] \tag{A.37}$$

$$N_{xs} = D\left(\frac{1-\nu}{2}\right)\left[u_{,s} + v_{,x}\right] + K\left(\frac{1-\nu}{2}\right)\left(\frac{1}{r}\right)\left[w_{,xs} + \left(\frac{1}{r}\right)v_{,x}\right] \tag{A.38}$$

$$N_{sx} = D\left(\frac{1-\nu}{2}\right)\left[u_{,s} + v_{,x}\right] - K\left(\frac{1-\nu}{2}\right)\left(\frac{c}{r}\right)\left[w_{,xs} - \left(\frac{1}{r}\right)u_{,s}\right] \tag{A.39}$$

$$N_s = D\left[v_{,s} - \frac{w}{r} - \nu u_{,x}\right] - K\left(\frac{c}{r}\right)\left[w_{,ss} + \frac{w}{r^2} - \left(\frac{1}{r^2}\right)(r_{,s})\,v\right] \tag{A.40}$$

$$M_x = -K\left[w_{,xx} + \nu w_{,ss} + \nu\left(\frac{v}{r}\right)_{,s} + \left(\frac{1}{r}\right)u_{,x}\right] \tag{A.41}$$

$$M_{xs} = K(1-\nu)\left[w_{,xs} + \left(\frac{1}{r}\right)v_{,x}\right] \tag{A.42}$$

$$M_{sx} = -K\left(\frac{1-\nu}{2}\right)\left[(1+c)\,w_{,xs} + \left(\frac{1}{r}\right)v_{,x} - \left(\frac{c}{r}\right)u_{,s}\right] \tag{A.43}$$

$$M_s = -K\left[cw_{,ss} + c\left(\frac{w}{r^2}\right) - \left(\frac{c}{r^2}\right)(r_{,s})\,v + \nu w_{,xx}\right] \tag{A.44}$$

and from Equations A.15 and A.16

$$Q_x = -K\Big\{w_{,xxx} + 1/2\,[1 + \nu + c\,(1 + \nu)]\,w_{,xss} + \frac{1-\nu}{2}\,c_{,s}\,w_{,xs} + \frac{1}{r}\,u_{,xx} - \frac{1-\nu}{2}\left[\frac{c}{r}\,u_{,s}\right]_{,s} + \frac{1+\nu}{2}\left(\frac{v}{r}\right)_{,xs}\Big\} \qquad (A.45)$$

$$Q_s = -K\Big\{cw_{,sss} + w_{,xxs} + c_{,s}\,w_{,ss} + c_{,s}\left(\frac{w}{r^2}\right) - c_{,s}\left(\frac{1}{r^2}\right)(r_{,s})\,v + c\left(\frac{w}{r^2}\right)_{,s} + \frac{1+\nu}{r}\,v_{,xx} - \left[\frac{c}{r^2}\,(r_{,s})\,v\right]_{,s}\Big\} \qquad (A.46)$$

where

$$D = \frac{Eh}{1-\nu^2}$$

$$K = \frac{Eh^3}{12\,(1-\nu^2)}$$

$$c = 12\left(\frac{r}{h}\right)^2\left\{\frac{r}{h}\log\left[\frac{1 + \frac{h}{2r}}{1 - \frac{h}{2r}} - 1\right]\right\} \doteq 1$$

Substitution of these stress resultants into the equilibrium equations in terms of the stress resultants and using c=1 gives the final form of the equilibrium equations. These equations are recorded in Chapter 2 as Equations 2.1. Note that these equilibrium equations are three coupled partial differential equations in u, v, and w with variable coefficients, in which

$$u = u\ (x,s)$$

$$v = v\ (x,s)$$

$$w = w\ (x,s)$$

$$r = r\ (s)$$

A.5 Donnell's Partial Differential Equations of Equilibrium

In addition to the assumptions in A.1 Donnell (3) made the following assumptions to derive a simplified set of equilibrium equations:

1. The transverse shearing force, Q_s (Figure 17) makes a negligible contribution to the equilibrium of forces in the circumferential direction.

2. The changes in curvature and twist are negligibly affected by the tangential displacement, v.

These assumptions reduce the stress resultants in Equations A.37 through A.44 to the following

$$N_x = D\left[u_{,x} + \nu v_{,s} - \nu \frac{w}{r}\right] \tag{A.47}$$

$$N_{xs} = N_{sx} = D\left(\frac{1-\nu}{2}\right)\left[u_{,s} + v_{,x}\right] \tag{A.48}$$

$$N_s = D\left[v_{,s} - \frac{w}{r} + \nu u_{,x}\right] \tag{A.49}$$

$$M_x = -K\left[w_{,xx} + \nu w_{,xx}\right] \tag{A.50}$$

$$M_{xs} = M_{sx} = K\,(1-\nu)\,w_{,xs} \tag{A.51}$$

$$M_{s} = -\,K\left[w_{,ss} + \nu w_{,xx}\right] \tag{A.52}$$

Donnell's assumptions also reduce Equation A.17 to

$$N_{s,s} + N_{xs,x} = -\,P_{s} \tag{A.53}$$

Substituting the stress resultants A.47 through A.52 into the equilibrium equations A.1, A.53, and A.18 gives the Donnell equations of equilibrium (Equations 2.4).

APPENDIX B

FINITE DIFFERENCE QUOTIENTS

The finite difference approximations used in this study are tabulated term by term (except for duplication) for each of the Equations 2.3 below. Note, the approximations are given in terms of point i, j in the discrete system.

$$u,_{\zeta\zeta}\Big|_{i,j} \longleftrightarrow \frac{1}{\Delta\zeta^2}\left[u_{i+1,j} - 2u_{i,j} + u_{i-1,j}\right]$$

$$u,_{\eta\eta}\Big|_{i,j} \longleftrightarrow \frac{1}{\Delta\eta^2}\left[u_{i,j+1} - 2u_{i,j} + u_{i,j-1}\right]$$

$$v,_{\zeta\eta}\Big|_{i,j} \longleftrightarrow \frac{1}{2\Delta\zeta\Delta\eta}\left[v_{i+1,\,j+1} - v_{i+1,\,j-1} - v_{i-1,\,j+1} + v_{i-1,\,j-1}\right]$$

$$\left(\frac{\ell}{r}\right)w,_{\zeta}\Big|_{i,j} \longleftrightarrow \frac{1}{2\Delta\zeta}\left[w_{i+1,j} - w_{i-1,j}\right]\left(\frac{\ell}{r}\right)_j$$

$$\left(\frac{\ell}{r}\right)w,_{\zeta\zeta\zeta}\Big|_{i,j} \longleftrightarrow \frac{1}{2\Delta\zeta^3}\left[w_{i+2,j} - 2w_{i+1,j} + 2w_{i-1,j} - w_{i-2,j}\right]\left(\frac{\ell}{r}\right)_j$$

$$\left[\left(\frac{\ell}{r}\right) w_{,\zeta\eta}\right]_{,\eta}\Big|_{i,j} \longleftrightarrow \frac{1}{4\Delta\zeta\Delta\eta^2}\left\{\left(\frac{\ell}{r}\right)_{j+1}\left[w_{i+1,\,j+2} - w_{i+1,j}\right.\right.$$

$$\left. - w_{i-1,\,j+2} + w_{i-1,j}\right]$$

$$\left. - \left(\frac{\ell}{r}\right)_{j-1}\left[w_{i+1,j} - w_{i+1,\,j-2} - w_{i-1,j} + w_{i-1,\,j-2}\right]\right\}$$

$$\left[\left(\frac{\ell}{r}\right)^2 u_{,\eta}\right]_{,\eta}\Big|_{i,j} \longleftrightarrow \frac{1}{4\Delta\eta^2}\left\{\left(\frac{\ell}{r}\right)^2_{j+1}\left[u_{i,\,j+2} - u_{i,j}\right]\right.$$

$$\left. - \left(\frac{\ell}{r}\right)_{j-1}\left[u_{i,j} - u_{i,\,j-2}\right]\right.$$

The terms $v_{,\eta\eta}$, $v_{,\zeta\zeta}$, $u_{,\zeta\eta}$ are similar to the terms $u_{,\eta\eta}$, $u_{,\zeta\zeta}$, $v_{,\zeta\eta}$, respectively.

$$\left[\left(\frac{\ell}{r}\right)w\right]_{,\eta}\Big|_{i,j} \longleftrightarrow \frac{1}{2\Delta\eta}\left[\left(\frac{\ell}{r}\right)_{j+1} w_{i,\,j+1} - \left(\frac{\ell}{r}\right)_{j-1} w_{i,\,j-1}\right]$$

$$\left(\frac{\ell}{r}\right)^2 v_{,\zeta\zeta}\Big|_{i,j} \longleftrightarrow \frac{1}{\Delta\zeta^2}\left[v_{i+1,j} - 2v_{i,j} + v_{i-1,j}\right]\left(\frac{\ell}{r}\right)^2_j$$

$$\left(\frac{\ell}{r}\right) w_{,\zeta\zeta\eta}\Big|_{i,j} \longleftrightarrow \frac{1}{2\Delta\zeta^2\Delta\eta}\left[w_{i+1,\,j+1} - 2w_{i,\,j+1}\right.$$

$$\left. + w_{i-1,\,j-1} - w_{i+1,\,j-1} + 2w_{i,\,j-1} - w_{i-1,\,j-1}\right]\left(\frac{\ell}{r}\right)_j$$

$$\left[\left(\frac{\ell}{r}\right)^2\left(\frac{r}{\ell}\right)_{,\eta} w_{,\eta\eta}\right]\Big|_{i,j} \longleftrightarrow \frac{1}{2\Delta\eta^3}\left(\frac{\ell}{r}\right)^2_j\left[\left(\frac{r}{\ell}\right)_{j+1} - \left(\frac{r}{\ell}\right)_{j-1}\right]$$

$$\left[w_{i,\,j+1} - 2w_{i,j} + w_{i,\,j-1} \right]$$

$$\left[\left(\frac{\ell}{r}\right)^4 \left(\frac{r}{\ell}\right)_{,\eta} w \right]\Bigg|_{i,j} \longleftrightarrow \frac{1}{2\Delta\eta} \left(\frac{\ell}{r}\right)_j^4 \left[\left(\frac{r}{\ell}\right)_{j+1} - \left(\frac{r}{\ell}\right)_{j-1} \right] w_{i,j}$$

$$\left\{ \left(\frac{\ell}{r}\right)^4 \left[\left(\frac{r}{\ell}\right)_{,\eta} \right]^2 v \right\}\Bigg|_{i,j} \longleftrightarrow \frac{1}{4\Delta\eta^2} \left(\frac{\ell}{r}\right)_j^4 \left[\left(\frac{r}{\ell}\right)_{j+1} - \left(\frac{r}{\ell}\right)_{j-1} \right]^2 v_{i,j}$$

$$w_{,\eta\eta\eta\eta}\Big|_{i,j} \longleftrightarrow \frac{1}{\Delta\eta^4} \left[w_{i,\,j+2} - 4w_{i,\,j+1} + 6w_{i,j} - 4w_{i,\,j-1} + w_{i,\,j-2} \right]$$

$$w_{,\zeta\zeta\zeta\zeta}\Big|_{i,j} \longleftrightarrow \frac{1}{\Delta\zeta^4} \left[w_{i+2,\,j} - 4w_{i+1,\,j} + 6w_{i,j} - 4w_{i-1,\,j} + w_{i-2,\,j} \right]$$

$$w_{,\zeta\zeta\eta\eta}\Big|_{i,j} \longleftrightarrow \frac{1}{\Delta\zeta^2\Delta\eta^2} \left[w_{i+1,\,j+1} - 2w_{i+1,j} + w_{i+1,\,j-1} - 2w_{i,\,j+1} + 4w_{i,j} - 2w_{i,\,j-1} + w_{i-1,\,j+1} - 2w_{i-1,\,j} + w_{i-1,\,j-1} \right]$$

$$\left(\frac{\ell}{r}\right)^2 w_{,\eta\eta}\Big|_{i,j} \longleftrightarrow \frac{1}{\Delta\eta^2} \left(\frac{\ell}{r}\right)_j^2 \left[w_{i,\,j+1} - 2w_{i,j} + w_{i,\,j-1} \right]$$

$$\left[\left(\frac{\ell}{r}\right)^2 w\right]_{,\eta\eta}\Big|_{i,j} \longleftrightarrow \frac{1}{2\Delta\eta}\left[\left(\frac{\ell}{r}\right)^2_{j+1} w_{i,j+1} - 2\left(\frac{\ell}{r}\right)^2_{j} w_{i,j} + \left(\frac{\ell}{r}\right)^2_{j-1} w_{i,j-1}\right]$$

$$\left(\frac{\ell}{r}\right)^4 w\Big|_{i,j} \longleftrightarrow \left(\frac{\ell}{r}\right)^4_{j} w_{i,j}$$

$$\left(\frac{\ell}{r}\right) u_{,\zeta\zeta\zeta}\Big|_{i,j} \longleftrightarrow \frac{1}{2\Delta\zeta^3}\left(\frac{\ell}{r}\right)_j \left[u_{i+2,j} - 2u_{i-i,j} - u_{i-2,j}\right]$$

$$\left|\left(\frac{\ell}{r}\right) u_{,\zeta\eta}\right|_{,\eta}\Big|_{i,j} \longleftrightarrow \frac{1}{8\Delta\zeta\Delta\eta^2}\left\{\left(\frac{\ell}{r}\right)_{j+1}\left[u_{i+1,\,j+2} - u_{i+1,j} - u_{i-1,\,j+2} + u_{i-1,\,j}\right] + \left(\frac{\ell}{r}\right)_{j-1}\left[u_{i+1,j} - u_{i+1,\,j-2} - u_{i-1,j} + u_{i-1,\,j-2}\right]\right\}$$

$$\left[\left(\frac{\ell}{r}\right) v_{\zeta\zeta}\right]_{,\eta}\Big|_{i,j} \longleftrightarrow \frac{1}{2\Delta\zeta^2\Delta\eta}\left\{\left(\frac{\ell}{r}\right)_{j+1}\left[v_{i+1,\,j+1} - 2v_{i,\,j+1} + v_{i-1,\,j+1}\right] + \left(\frac{\ell}{r}\right)_{j-1}\left[v_{i+1,\,j-1} - 2v_{i,\,j-1} + v_{i-1,\,j-1}\right]\right\}$$

$$\left[\left(\frac{\ell}{r}\right)^2 \left(\frac{r}{\ell}\right)_{,\eta} v\right]_{,\eta\eta}\Big|_{i,j} \longleftrightarrow \frac{1}{2\Delta\eta^3}\left\{\left(\frac{\ell}{r}\right)^2_{j+1}\left[\left(\frac{r}{\ell}\right)_{J+2} - \left(\frac{r}{\ell}\right)_{j}\right] v_{i,\,j+1}\right.$$

$$- 2\left(\frac{\ell}{r}\right)^2_j \left[\left(\frac{r}{\ell}\right)_{j+1} - \left(\frac{r}{\ell}\right)_{j-1}\right] v_{i,j}$$

$$+ \left(\frac{\ell}{r}\right)_{j-1} \left[\left(\frac{r}{\ell}\right)_{j} - \left(\frac{r}{\ell}\right)_{j-2}\right] v_{i,\,j-1} \Bigg\}$$

$$\left[\left(\frac{\ell}{r}\right)^4 \left(\frac{r}{\ell}\right)_{,\eta} v\right]\Bigg|_{i,j} \longleftrightarrow \frac{1}{2\Delta\eta}\left(\frac{\ell}{r}\right)^4_j \left[\left(\frac{r}{\ell}\right)_{j+1} - \left(\frac{r}{\ell}\right)_{j-1}\right] v_{i,j}$$

$$\left(\frac{\ell}{r}\right) v_{,\eta}\Big|_{i,j} \qquad \frac{1}{2\Delta\eta}\left(\frac{\ell}{r}\right)_j \left[v_{i,j+1} - v_{i,j-1}\right]$$

$$\left(\frac{\ell}{r}\right)^2 w\Big|_{i,j} \longleftrightarrow \left(\frac{\ell}{r}\right)^2_j w_{i,j}$$

$$\left(\frac{\ell}{r}\right) u_{,\zeta}\Big|_{i,j} \longleftrightarrow \frac{1}{2\Delta\zeta}\left(\frac{\ell}{r}\right)_j \left[u_{i+1,j} - u_{i-1,j}\right]$$

VITA

Jimmie D. Ramey

Candidate for the Degree of

Doctor of Philosophy

Thesis: A NUMERICAL ANALYSIS OF NONCIRCULAR CYLINDRICAL SHELLS

Major Field: Engineering

Biographical:

Personal Data: Born September 25, 1933, in Springfield, Missouri, the son of James H. and Freida E. Ramey.

Education: Graduate from Central High School, Tulsa, Oklahoma, in May, 1951; received the degree of Bachelor of Science in Civil Engineering from Oklahoma State University in August, 1960; received the degree of Master of Science from Oklahoma State University in August, 1962; completed requirements for the degree of Doctor of Philosophy from Oklahoma State University in August 1969.

Professional Experience: Part-time engineering aid for the Soil Conservation Service, June 1959-June 1961; part-time instructor for the School of Civil Engineering, June 1961-June 1964; research engineer for North American Aviation, Tulsa, June 1964-September 1965; instructor for the School of Civil Engineering, September 1965-January 1968; research engineer for The Boeing Co., Wichita, January 1968 to present time. Registered Professional Engineer in the State of Oklahoma.